発表者氏名	論文タイトル名	発表誌名	巻号	ページ	出版年
Tsurusaki Y, et al., Matsumoto N.	Mutations affecting components of the SWI/SNF complex cause Coffin-Siris syndrome.	Nat Genet	44(4)	376-378	2012
Saitsu H, et al., Matsumoto N.	Whole exome sequenwcing identifies KCNQ2 mutations in Ohtahara syndrome.	Ann Neurol	72(2)	298-300	2012
Miyake N, et al., Matsumoto N.	*KDM6A* point mutations cause Kabuki syndrome	Hum Mut	34(1)	108-110	2013

CONTEMPORARY NEUROLOGY SERIES
PREVIOUS VOLUMES

SERIES EDITOR
Sid Gilman, MD, FRCP
William J. Herdman Distinguished University Professor of Neurology, University of Michigan

Volume 76
PARANEOPLASTIC SYNDROMES
Robert B. Darnell, MD, PhD, and Jerome B. Posner, MD, FAAN

Volume 75
THE NEURONAL CEROID LIPOFUSCINOSES (BATTEN DISEASE)
Second Edition
Sara E. Mole, PhD, Ruth E. Williams, MD, and Hans H. Goebel, MD

Volume 77
CLINICAL NEUROPHYSIOLOGY OF THE VESTIBULAR SYSTEM
Fourth Edition
Robert W. Baloh, MD, FAAN, and Kevin A. Kerber, MD

Volume 78
PERIPHERAL NEUROPATHIES IN CLINICAL PRACTICE
Steven Vinkovitz, MD, Stephen N. Scelsa, MD, and Herbert H. Schaumburg, MD

Volume 79
CLINICAL NEUROPHYSIOLOGY
Third Edition
Jasper R. Daube, MD, and Devon I. Rubin, MD, Editors

Volume 74
NEUROLOGICAL COMPLICATIONS OF CRITICAL ILLNESS
Third Edition
Eelco F.M. Wijdicks, MD, PhD, FACP

Volume 73
NEUROLOGIC COMPLICATIONS OF CANCER
Second Edition
Lisa M. DeAngelis, MD, and Jerome B. Posner, MD

Volume 72
PRINCIPLES OF DRUG THERAPY IN NEUROLOGY
Second Edition
Michael V. Johnston, MD, and Robert A. Gross, MD, Editors

Volume 71
PLUM AND POSNER'S DIAGNOSIS OF STUPOR AND COMA
Fourth Edition
Jerome B. Posner, MD, Clifford B. Saper, MD, PhD, Nicholas D. Schiff, MD, and Fred Plum, MD

Volume 70
THE NEUROLOGY OF EYE MOVEMENTS
Fourth Edition
R. John Leigh, MD, FRCP, and David S. Zee, MD

ADVANCE PRAISE FOR *JASPER'S BASIC MECHANISMS OF THE EPILEPSIES, FOURTH EDITION*

"This is a masterfully selected comprehensive collection of topics all closely related to seizures themselves. Most fittingly . . . the editors have taken the opportunity of the publication of this [fourth] edition to uphold a long-standing and powerful tradition for this series. They provide not only a historical perspective on Jasper and his lasting influence on epilepsy research, but also carefully identify current and future issues for the field. . . . The utility of this volume is then made evident by the fact that all such advances will rely on the basic principles outlined in this timely publication." —**John Huguenard, PhD, Department of Neurology and Neurological Sciences, Stanford University School of Medicine, Stanford, CA**

"The original *Basic Mechanisms of the Epilepsies* by Jasper, Ward, and Pope was a compendium of the best and brightest research of the late 1960s and an inspiration to that generation of investigators. This present book has achieved the same result. The view of the basic mechanisms uncovered by that era of epilepsy researchers has now blossomed into an even more complicated and fascinating picture of the fundamentals of epilepsy, well described by this large group of world-class experts." —**Peter L. Carlen MD, FRCPC, Departments of Medicine (Neurology), Physiology, and IBBME, University of Toronto, ON, Canada**

ISBN 978-0-19-974654-5
90000
9 780199 746545

OXFORD
UNIVERSITY PRESS
www.oup.com

NOEBELS • AVOLI
ROGAWSKI • OLSEN
DELGADO-ESCUETA

JASPER'S
BASIC MECHANISMS
OF THE EPILEPSIES

FOURTH EDITION

OXFORD

80

CONTEMPORARY NEUROLOGY SERIES

JASPER'S BASIC MECHANISMS OF THE EPILEPSIES

FOURTH EDITION

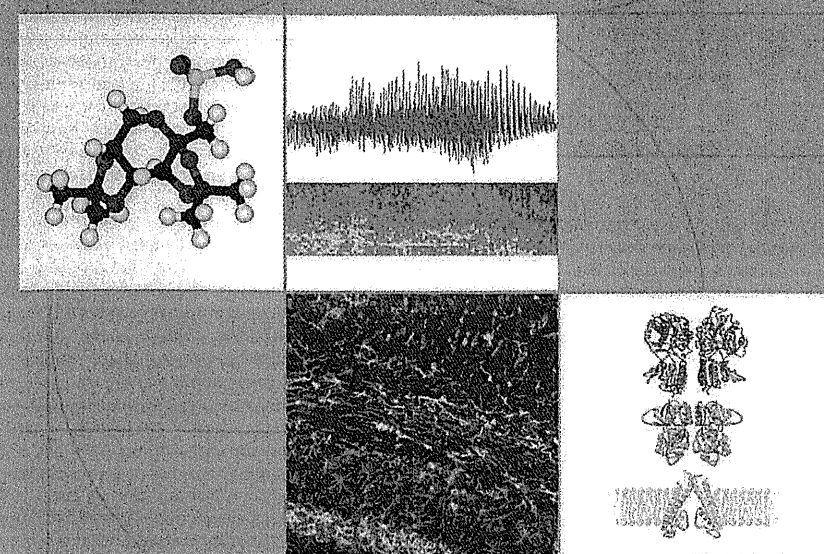

JEFFREY L. NOEBELS, MASSIMO AVOLI
MICHAEL A. ROGAWSKI, RICHARD W. OLSEN
ANTONIO V. DELGADO-ESCUETA

OXFORD

Chapter 64

Haploinsufficiency of *STXBP1* and Ohtahara Syndrome

Hirotomo Saitsu
Mitsuhiro Kato
Naomichi Matsumoto

INTRODUCTION

Ohtahara syndrome (OS), also known as *early infantile epileptic encephalopathy with suppression-burst*, is one of the most severe and earliest forms of epilepsy.[1] It is characterized by early onset of tonic seizures, seizure intractability, characteristic suppression-burst patterns on the electroencephalogram (EEG), and a poor outcome with severe psychomotor retardation.[2,3] Brain malformations, such as cerebral dysgenesis or hemimegalencephaly, are often associated with OS, but cryptogenic or idiopathic OS is found in a subset of OS patients, in whom genetic aberrations might be involved.[4] Although mutations of the *ARX* gene have been found in several male patients with OS,[5–8] the genetic causes are unexplained in most cryptogenic OS cases. We have recently found de novo mutations in *STXBP1* (encoding syntaxin binding protein 1, also known as MUNC18-1) in individuals with cryptogenic OS.[9] Here we present all the mutations in *STXBP1* found to date in OS patients, as well as some evidence of mutations leading to haploinsufficiency.

OHTAHARA SYNDROME

Ohtahara syndrome was first reported as the earliest form of age-dependent epileptic syndromes by Ohtahara et al.[1] It is characterized by early onset of intractable tonic spasms, characteristic suppression-burst patterns on interictal EEG, and a poor outcome with severe psychomotor retardation.[2,3] According to a previous report,[4] all patients have seizure onset within the first 3 months, with the majority (75%) in the first month. Tonic spasms were observed in all patients. One-third to one-half of patients also had partial seizures, such as erratic focal motor seizures and hemiconvulsions, or asymmetric tonic seizures; however, myoclonic seizures were rare. Hemiconvulsions, tonic seizures, or clonic seizures precede the onset of tonic spasms by 1 to several weeks to in 37.5% of OS patients.[4] Brain malformations, such as cerebral dysgenesis, hemimegalencephaly, porencephaly, and Aicardi syndrome, are often associated with OS, but a significant proportion of patients (31% to 50% of OS cases) remain etiologically unexplained.[2,4] Suppression-burst patterns on interictal EEG consisting of high-voltage activity alternating with nearly flat suppression phases are observed when the patient is both awake and asleep.

Early myoclonic encephalopathy (EME) is another epileptic syndrome showing suppression-burst patterns on EEG.[10] The prevailing initial seizure type is a main difference between OS and EME: tonic seizures in OS and myoclonic seizures in EME.[2,3] However, OS and EME have common features, and it is often difficult to distinguish between them. Homozygous missense mutations of the *SLC25A22* (mitochondrial glutamate carrier 1) gene have been recently found in EME individuals in consanguineous families.[11,12] Age-dependent evolution is a characteristic feature of both OS and EME: approximately 75% and 40% of OS and EME cases, respectively, transit to West syndrome (WS), usually 3–4 months afterward.[2,3] West syndrome is characterized by tonic spasms with clustering, arrest of psychomotor development, and hypsarrhythmia on EEG. Such transitions suggest a common pathophysiology between OS and WS or between EME and WS. Consistent with this hypothesis, specific mutations of the *ARX* (*aristaless*-related homeobox) gene at Xp22.13, have been recently found in male OS and WS cases.[5–8,13–15]

DE NOVO *STXBP1* MUTATIONS CAUSE OS

Identification of *STXBP1* Mutations in Patients with OS

Through BAC array-based comparative genomic hybridization analysis of patients associated with mental retardation (MR), we found a microdeletion at 9q33.3-q34.11 in a female patient with OS.[9] As the microdeletion occurred de novo, we assumed that a gene within the deletion was responsible for OS. Among the genes mapped within the deletion, the gene encoding syntaxin binding protein 1 (STXBP1) was of particular interest because mouse *Stxbp1* has been shown to be essential for synaptic vesicle release[16] and is specifically expressed in the brains of rodents and humans.[17,18] We therefore analyzed *STXBP1* in 13 unrelated patients with OS. Four heterozygous missense mutations were found at evolutionarily conserved amino acids in three males and one female (Fig. 64–1 and Table 64–1). Three mutations were confirmed as de novo events (paternal DNA was unavailable for one remaining mutation).

STXBP1 Mutation Is a Major Genetic Cause of OS

To delineate the clinical spectrum of patients with *STXBP1* mutations, *STXBP1* was further analyzed in 29 and 54 cases of cryptogenic OS and WS, respectively.[19] No brain malformations were found in any of the cases. Seven novel heterozygous mutations were found in nine OS cases (the same mutation was found in three cases), but none in WS cases (six males and three females; Fig. 64–1 and Table 64–1). The mutations included one missense, one splicing, two frameshift, and three nonsense mutations. A recurrent missense mutation (c.1217G>A, p.R406H) occurred at an evolutionarily conserved amino acid (Fig. 64–1). All the mutations occurred de novo. Collectively, *STXBP1* aberrations account for about one-third of individuals with OS (14 out of 43). These data showed that *STXBP1* mutations are a major genetic cause of cryptogenic OS, but they are not a genetic cause of WS in our Japanese cohort.

Clinical Features of Patients with *STXBP1* Deletion/Mutations

Clinical information from 14 individuals with confirmed *STXBP1* deletion/mutations is summarized in Table 64–1. These persons showed

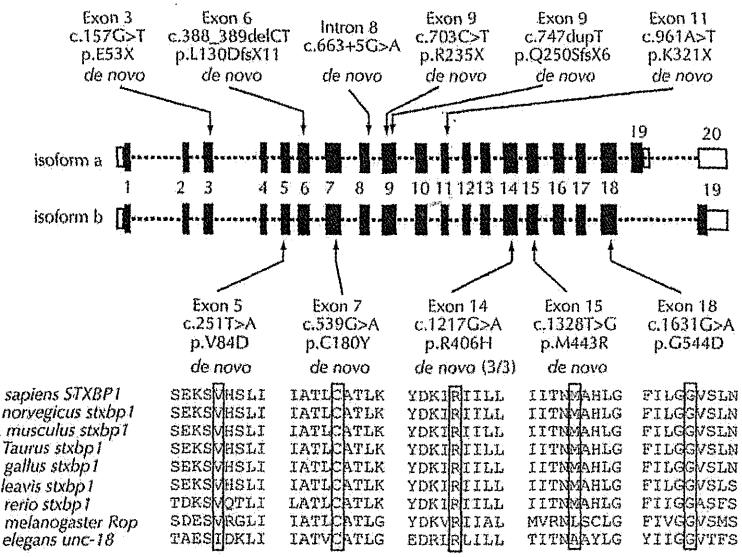

Figure 64–1. Summary of *STXBP1* mutations found in Japanese individuals with OS. Schematic representation of STXBP1, consisting of at most 20 exons (the UTR and the coding region are open and filled rectangles, respectively). There are two isoforms, a (GenBank accession number, NM_003165) with exon 19, and b (NM_001032221) without exon 19 of isoform a. Locations of mutations are indicated by arrows. Eleven different mutations are presented; missense mutations are indicated below the gene scheme, and the other types of mutations are indicated above the gene. Ten mutations in 12 subjects occurred de novo. All missense mutations occurred at evolutionarily conserved amino acids. CLUSTALW (http://align.genome.jp/) was used to align homologs of different species. Adapted from refs. 9 and 19.

distinctive features of OS, such as early-onset seizures including epileptic spasms, suppression-burst pattern on EEG, transition to WS after a few to several months, and severe developmental delay. Epileptic spasms were preceded by other seizure types, including partial seizures in 11 subjects. Transition to WS was observed in 11 subjects with OS. Although seizures were intractable in nine subjects, five subjects responded to medication, such as thyrotropin-releasing hormone (TRH) injection, adrenocorticotropic hormone (ACTH) injection, vitamin B_6, high-dose phenobarbital, and valproic acid. All subjects demonstrated severe psychomotor developmental delay. Brain magnetic resonance imaging (MRI) showed no structural anomalies or hippocampal anomalies but did show some atrophy (Fig. 64–2A). Suppression-burst on interictal EEG was observed in both awake and asleep states (Fig. 64–2B). We gained several insights into the phenotype of *STXBP1* aberrations. Firstly, the age at onset of epileptic spasms is later in subjects with *STXBP1* aberrations than in the 16 original subjects reported by Yamatogi and Ohtahara.[4] Only 27% of the subjects (4/15) in our series had onset of OS within 1 month compared to 75% (12/16) in the series of Yamatogi and Ohtahara. As subjects with *STXBP1* aberrations showed no structural anomalies on brain MRI examination, the onset of epileptic seizures might be affected by associated structural brain abnormalities, which are commonly seen in other reports of OS. Secondly, myoclonic seizures, which are thought to be rarely observed in OS, were occasionally observed (3/14). Myoclonic seizures are the main ictal symptom of EME. These three subjects can be diagnosed as having EME when myoclonic seizures dominate. Thus, *STXBP1* might also be causative for EME, implying a genetic linkage between OS and EME. Another infrequent but interesting finding is that one patient (no. 5) developed vigorous chorea-ballismus

Table 64–1 Summary of Clinical Features of Subjects with STXBP1 Deletion/Mutations

Case # Mutation	Initial Symptoms	Onset of Spasms	Transition from Spasms to Other Seizures	Response to Therapy
#1 Deletion	Tonic seizure and oral automatism	2 m	Generalized clonic seizure at 29 m	Seizure free from 5 m after TRH injection
#2 c.1631G>A	Blinking	10 d	No	Seizure free from 3 m
#3 c.539G>A	Tonic seizure with blinking	3 m	No	Intractable, daily
#4 c.1325T>G	Upward gazing and tonic seizure	2 m	Partial seizure at 8 m	Intractable, hourly TRH injection was temporally effective
#5 c.251T>A	Spasms and tonic-clonic seizure	2 m	No	Intractable, daily
#6 c.1217G>A	Generalized convulsions	3 w	No	Intractable, hourly
#7 c.1217G>A	GTCS with upward eye gazing	2 m	Myoclonic seizure at 45 d	Intractable, daily
#8 c.1217G>A	Partial seizures (right hemiconvulsion)	2 m	Tonic seizure to myoclonic seizure	Intractable, daily
#9 c.157G>T	Spasms	2 d	Versive seizure after hypoxia at 2 y	Intractable, daily
#10 c.388_389del	Secondary generalized seizures	2 m	CPS	Seizure free after ACTH or VPA with KBr
#11 c.663+5G>A	Blinking to tonic seizures	1 m	Tonic seizure	Seizure free with VB6 for spasms and ACTH for WS
#12 c.703C>T	Spasms in cluster	1 m	No	Seizure free from 6 m after high-dose PB
#13 c.747dup	Clonic convulsion	31 d	Partial seizure and myoclonic seizures	Intractable, hourly
#14 c.961A>T	Partial seizures	3 w	Partial seizure	Intractable, daily

GTCS, generalized tonic-clonic seizures; CPS, complex partial seizure; TRH, thyrotropin-releasing hormone; ACTH, adrenocorticotropic hormone; VPA, valproic acid; KBr, potassium bromide; VB6, vitamin B_6; PB, phenobarbital; d, day(s); w, week; m, month(s); y, year(s); 0 w, 0 to 6 days; 0 m, 0 to 3 weeks.

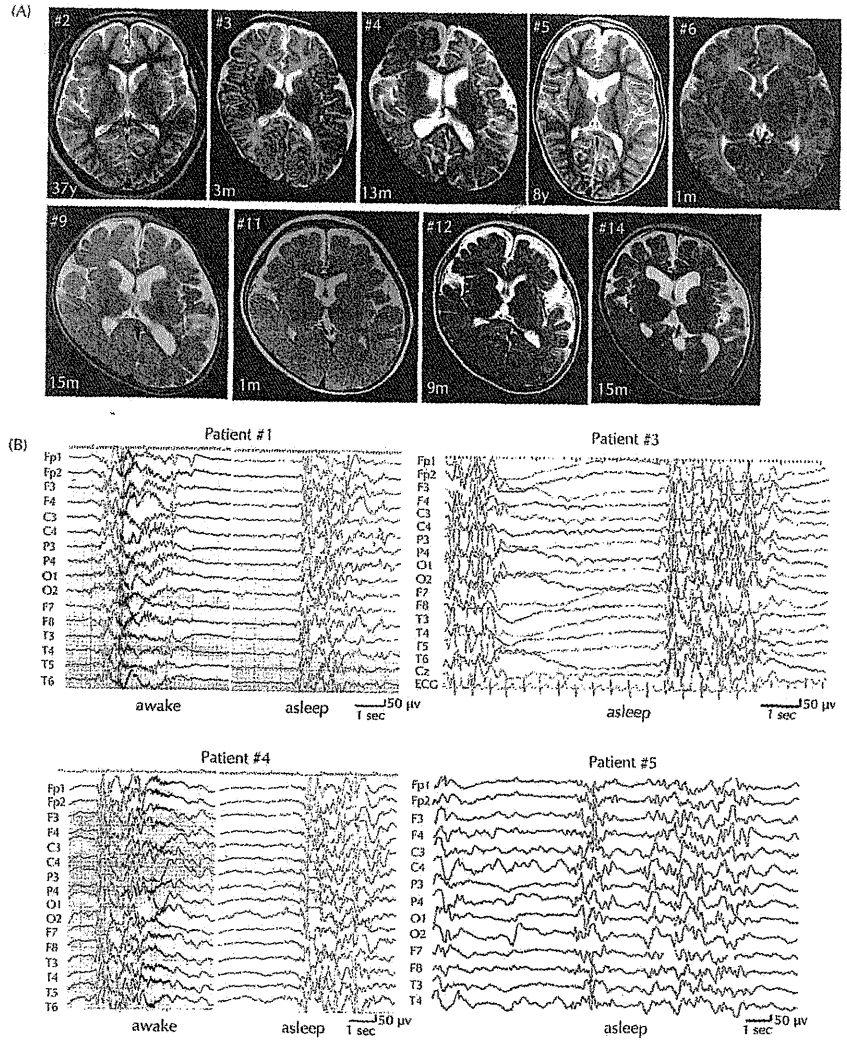

Figure 64–2. Brain MRI scan and EEG of OS patients with *STXBP1* aberrations. **A.** Brain MRI (T2-weighted axial) image through the basal ganglia shows normal brain structure in patients with *STXBP1* mutations. Patient IDs and developmental stages are indicated. Mild dilatation of lateral ventricles is observed in patients #4, #9, #11, and #14, but none shows brain malformation. y, year(s); m, month(s). **B.** Suppression-burst on interictal EEG of patients 1 (at age 2 months), 3 (at 3 months), 4 (at 2 months), and 5 (at 3 months). High-voltage bursts alternating with almost flat suppression phases at an approximately regular rate in both awake and asleep states. Adapted from refs. 9 and 19.

subsequent to OS, suggesting that mutations of *STXBP1* could affect the basal ganglia.[9,20] In terms of the genotype–phenotype relationship, we found no difference in clinical data between seven subjects with missense mutations and seven subjects with microdeletions, premature termination codons, or splicing mutations. This finding is supported by our experimental data that demonstrated both missense mutations and a splicing mutation resulted in haploinsufficiency of *STXBP1*: degradation of STXBP1 proteins containing missense mutations and nonsense-mediated mRNA decay (NMD) associated with aberrantly spliced mRNAs (see below).

MOLECULAR EVIDENCE OF *STXBP1* HAPLOINSUFFICIENCY

Mutant STXBP1 Proteins Are Unstable

All five missense mutations lead to amino acid replacements in the hydrophobic core of STXBP1 and are considered to destabilize the folding architecture. This is especially true for the three mutants (p.V84D, p.G544D, and p.M443R) that have replaced the wild-type (WT) residues with charged residues, which would be predicted to severely disrupt the conformation of STXBP1.[9] In fact, circular dichroism (CD) spectra showed that the helical content of the C180Y mutant is lower (39%) than that of the WT (43%), suggesting that the mutation destabilized the secondary structure of STXBP1[9] (Fig. 64–3A). Moreover, CD melting experiments revealed that the melting temperature (T_m) of the C180Y mutant was about 11 degrees lower than that of the WT (Fig. 64–3B), indicating that the C180Y mutant is much more unstable than the WT. The regulation of synaptic vesicle release by Stxbp1 is mediated in part by binding to Syntaxin-1A as well as directly to the soluble *N*-ethylmaleimide-sensitive factor attachment protein receptor (SNARE) complex, which mediates fusion of vesicles with the target membrane.[21,22] Binding of a mutant protein (p.C180Y) to syntaxin-1A was also significantly impaired, even at 4°C in vitro.[9] Together with the fact that the T_m of the C180Y mutant is close to the physiological temperature of the human body, it is less likely that its functional activity could be retained in the human brain. Other STXBP1 mutants (p.V84D, p.G544D, and p.M443R) tend to form aggregates, and thus sufficient protein for biophysical analyses could not be obtained.

Degradation of Mutant *STXBP1* Proteins

Transient expression of mutant STXBP1 proteins in Neuroblastoma 2A (N2A) cells showed further evidence of *STXBP1* haploinsufficiency. The WT EGFP-STXBP1 was expressed in the cytosolic compartment, but not in the nucleus or plasma membrane, similar to endogenous expression.[9,23] However, in approximately 20% of cells expressing mutant EGFP-STXBP1 (p.V84D, p.C180Y, p.M443R, and p.G544D), intense clusters of fluorescence signals were observed, likely representing protein aggregation.[9] The other 80% of cells showed a diffuse cytosolic protein distribution similar to that expressing the WT, but the signal intensity was much weaker, implying possible protein degradation. Protein degradation of mutant STXBP1 proteins was also confirmed by immunoblotting using an anti-Munc18 antibody[19] (Fig. 64–3C). These experiments suggested that mutant STXBP1 proteins would be aggregated or degraded in neurons, both leading to loss of STXBP1 function.

Degradation of *STXBP1* mRNA with Abnormal Splicing

The splicing, frameshift, and nonsense mutations would produce a premature stop codon; therefore, these mutant mRNAs are likely to be degraded by NMD.[24,25] In fact, NMD associated with abnormal splicing was demonstrated in lymphoblastoid cells derived from a patient harboring a c.663+5G>A mutation. Polymerase chain reaction (PCR) primers designed to amplify exons 7 to 10 amplified a single band (338 bp), corresponding to the WT *STXBP1* allele, using a cDNA template from a control lymphoblastoid cell lines (LCL; Fig. 64–3D). By contrast, a smaller band was detected from the patient's cDNA, in which exon 8 of *STXBP1* was skipped (Fig. 64–3D), resulting in the insertion of nine new amino

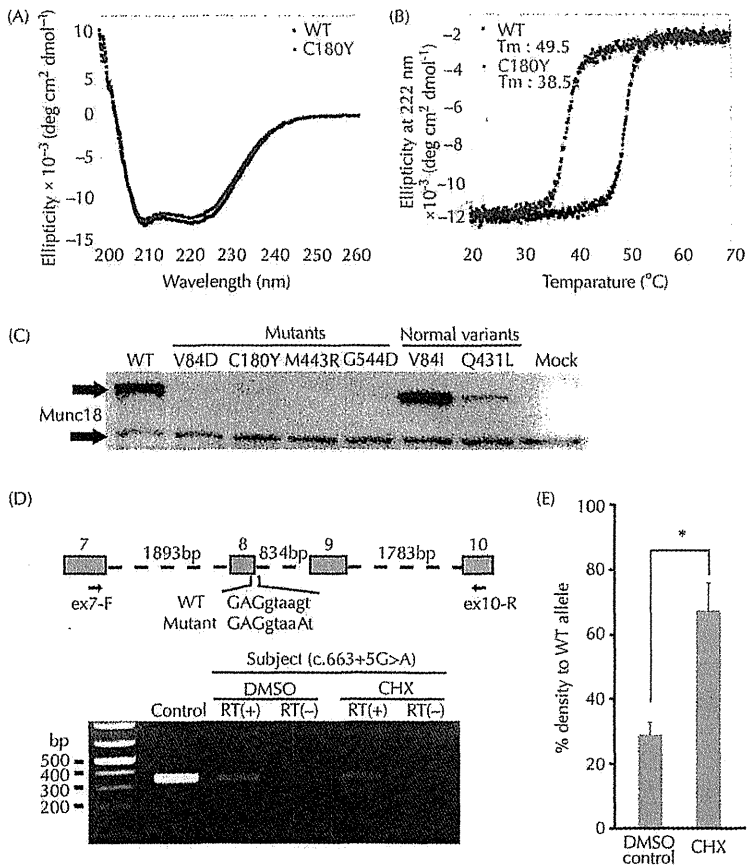

Figure 64–3. Characterization of mutant STXBP1 proteins and mRNAs with aberrant splicing. **A.** Circular dicroism spectra of the WT and C180Y-mutated STXBP1. The C180Y mutation is found to induce a subtle decrease in the helical contents of the STXBP1 structure by comparing the peaks of both proteins at 222 nm, where a large negative ellipticity value indicates a high helical content of the protein. **B.** Circular dicroic melting curves of the STXBP1 WT and C180Y proteins. Values of ellipticity at 222 nm are measured to monitor the thermal unfolding of the proteins. The C180Y mutant became unfolded at a lower temperature compared to the WT. Each dot represents the average of three repeated experiments, with standard deviations depicted as error bars. **C.** Immunoblot analysis of mutant STXBP1 proteins using a monoclonal anti-Munc18 antibody. Upper and lower bands represent EGFP-STXBP1 and endogenous STXBP1 proteins, respectively. Expression of four mutant STXBP1 proteins was not detected, while the WT and two normal variants could be detected. **D.** Top: Schematic representation of the genomic structure from exons 7 to 10 of *STXBP1*. Exons, introns, and primers are shown by boxes, dashed lines, and arrows, respectively. Sequences of exons and introns are presented in uppercase and lowercase, respectively. The mutation in intron 8 is highlighted in bold. Bottom: Reverse transcriptase-PCR analysis of patient 11 with a c.663+5G>A mutation and a normal control. Two PCR products were detected from the patient's cDNA: the upper one is the WT transcript and the lower one is the mutant. Only a single WT amplicon was detected in the control. The mutant amplicon was significantly increased by 30 μM cycloheximide (CHX) treatment compared to dimethyl sulfoxide (DMSO) treatment as a vehicle control. RT (+): with reverse transcriptase, RT (−): without reverse transcriptase as a negative control. **E.** Quantitative analysis of the NMD inhibition by CHX based on the data shown in **D.** $^*P = 0.0023$ by unpaired Student's *t*-test, two tailed. Averages of three repeated experiments are shown with error bars (s.d). Adapted from refs. 9 and 19.

acids followed by a premature stop codon at position 203. Moreover, the intensity ratio of the mutant compared to the normal band was increased by up to 67% after treatment with 30 μM cycloheximide, which inhibits NMD, compared to a ratio of 29% in the untreated condition (Fig. 64–3D,E). These facts suggest that the mutant mRNA possessing a premature stop codon suffered from degradation by NMD in neurons, resulting in haploinsufficiency.

Considering the degradation of STXBP1 proteins with missense mutations, NMD of mRNAs with premature stop codons and the effects of deletion of STXBP1, we conclude that haploinsufficiency of *STXBP1* causes OS.

HOW WOULD HAPLOINSUFFICIENCY OF *STXBP1* LEAD TO OS?

Impairment of Synaptic Vesicle Release

STXBP1 (*MUNC18-1*) is a member of the evolutionarily conserved Sec1/Munc-18 gene family that acts at specific steps of intracellular membrane transport.[26,27] In mammalian exocytosis, the vesicular SNARE protein, VAMP2 (also known as *synaptobrevin2*), and the target membrane SNARE proteins, Syntaxin-1 and SNAP25, constitute the core fusion machinery that bring two membranes into close apposition to fuse.[22,28] An *Stxbp1* null mutation led to complete loss of neurotransmitter secretion from synaptic vesicles throughout development in mice, though seizures have never been described.[16] Thus, *STXBP1* very likely plays a central role in synaptic vesicle release in coordination with SNARE proteins. The association of mutations of *STXBP1* with OS implies that perturbation of synaptic vesicle release forms part of the genetic basis of epilepsy. To date, the majority of genes associated with epilepsy syndromes are ion channel genes.[29] Synapsin I is a synaptic vesicle protein thought to regulate the kinetics of neurotransmitter release during priming of synaptic vesicles, and a mutation has been identified in a family with X-linked epilepsy and learning difficulties.[30] *STXBP1* is the second synaptic vesicle gene shown to be involved in epilepsy, and this finding will encourage further research into regulation of synaptic vesicle release and its involvement in seizures and related disorders.

Possible Interneuropathy

In *Stxbp1* heterozygous knockout mice, no seizures have been reported, and whole-cell recordings of autaptic glutamatergic or GABAergic (GABA: gamma-aminobutyric acid) neurons showed excitatory and inhibitory postsynaptic currents similar to those of WT littermate neurons upon single depolarizations.[31] However, with repeated stimulation, *Stxbp1*$^{+/-}$ neurons showed impaired synaptic function due to the reduced size and replenishment rate of readily releasable vesicles,[31] suggesting that heterozygous deletion of *Stxbp1* indeed affected synaptic function in mice. Interestingly, the reduction of readily releasable vesicles was more evident in GABAergic neurons than in glutamatergic neurons.[31] It has been reported that *Arx* is expressed in GABAergic interneurons and that *Arx* controls their genesis, migration, and differentiation, as *Arx* knockout mice showed a deficit of GABAergic interneurons.[32] Moreover, neuropathological examination of three patients with X-linked lissencephaly with absent corpus callosum and ambiguous genitalia, caused by *ARX* mutations, has suggested a loss of interneurons.[33] If haploinsufficiency of *STXBP1* affected GABAergic interneurons more severely than glutamatergic neurons in humans, as in mice, a defect in the GABAergic system could be postulated as a common pathophysiology among OS patients with *ARX* or *STXBP1* mutations. Ohtahara syndrome might be designated as a continuum of interneuronopathies.[34,35]

Cell Death of the Brainstem

As brain malformations are often associated with individuals with OS,[2,3] it could be speculated that *STXBP1* mutations would lead to abnormal brain structures directly related to the seizure phenotype of OS. However, we did not observe structural brain anomalies in any of the 14 OS patients with *STXBP1* defects. This is consistent with the findings that mice deleted for *Stxbp1* have normal brain architec-

ture. *Stxbp1* null mice, however, showed extensive cell death of mature neurons in lower brain areas, such as the brainstem; the lower brainstem was almost completely lost by embryonic day 18.[16] This is consistent with the suggestion that tonic seizures in OS might originate from subcortical structures, including the brainstem. Thus, in addition to the impaired synaptic vesicle release, it is possible that *STXBP1* haploinsufficiency leads to OS through microscopically impaired neuronal cell death in lower brain areas.

FUTURE CHALLENGES

Expansion of the Clinical Spectrum of *STXBP1* Mutations

Although OS is the core phenotype of *STXBP1* defects in our Japanese cohort (one-third of OS cases harbored *STXBP1* mutations), Hamdan et al. recently reported that two de novo *STXBP1* mutations, c.1162C>T (p.R388X) and c.169+1G>A, were identified in 2 out of 95 individuals with MR and nonsyndromic epilepsy.[36] According to their report, the two patients never showed the tonic seizures or infantile spasms associated with OS and WS, respectively. The onset of first seizures was at 6 weeks and 2 years of age, respectively. In addition, characteristic EEG patterns, such as suppression-burst or hypsarrhythmia, were never observed in these patients. Thus, the finding by Hamdan et al. indicated that *STXBP1* defects could cause a wide spectrum of clinical epileptic disorders in association with severe MR. Given that defects in synaptic dysfunction have also been implicated in many common neurodevelopmental disorders, such as MR, autism, and schizophrenia,[37,38] the possible involvement of *STXBP1* mutations in such common neurodevelopmental disorders is of interest. Elucidation of the molecular basis of synaptic vesicle processing disturbed by *STXBP1* mutations will allow us to understand not only the pathophysiology of infantile epilepsy, but also many neuropsychiatric conditions that present beyond childhood. The contribution of *STXBP1* mutations to EME also should be clarified, because myoclonic seizures, the characteristic feature of EME, are occasionally observed in 3/14 patients with *STXBP1* mutations.

Animal Model

An animal model is necessary to elucidate the pathophysiology of epilepsy caused by *STXBP1* mutations, including age dependency of seizure type and EEG pattern, and to test potential therapies directed specifically at OS and subsequent WS. The effect of gene dosage alterations of *STXBP1/Stxbp1* might vary between humans and mice: humans might be more susceptible than mice; thus, loss of function of one allele could cause seizures in humans but not in mice. Although it would be challenging to manipulate the gene dosage of *Stxbp1*—for example, in combination with a hypomorphic allele and a null allele—to the level at which mutant mice show a seizure phenotype, the establishment of an animal model will greatly benefit our understanding of the mechanisms of seizures in relation to impaired synaptic function.

DISCLOSURE STATEMENT

None of the authors have financial interests related to this work.

REFERENCES

1. Ohtahara S, Ishida T, Oka E, Yamatogi Y, Inoue H, Karita S, Ohtsuka Y. [On the specific age dependent epileptic syndrome: the early-infantile epileptic encephalopathy with suppression-burst.]. *No to Hattatsu*. 1976;8:270–279.
2. Djukic A, Lado FA, Shinnar S, Moshe SL. Are early myoclonic encephalopathy (EME) and the Ohtahara syndrome (EIEE) independent of each other? *Epilepsy Res*. 2006;70(suppl 1):S68–S76.
3. Ohtahara S, Yamatogi Y. Ohtahara syndrome: with special reference to its developmental aspects for differentiating from early myoclonic encephalopathy. *Epilepsy Res*. 2006;70(suppl 1):S58–S67.
4. Yamatogi Y, Ohtahara S. Early-infantile epileptic encephalopathy with suppression-bursts, Ohtahara syndrome; its overview referring to our 16 cases. *Brain Dev*. 2002;24:13–23.
5. Kato M, Saitoh S, Kamei A, Shiraishi H, Ueda Y, Akasaka M, Tohyama J, Akasaka N, Hayasaka K. A longer polyalanine expansion mutation in the ARX gene causes early infantile epileptic encephalopathy with suppression-burst pattern (Ohtahara syndrome). *Am J Hum Genet*. 2007;81:361–366.
6. Fullston T, Brueton L, Willis T, Philip S, MacPherson L, Finnis M, Cecz J, Morton J. Ohtahara syndrome in a family with an ARX protein truncation mutation (c.81C>G/p.Y27X). *Eur J Hum Genet*. 2010;18:157–162.
7. Absoud M, Parr JR, Halliday D, Pretorius P, Zaiwalla Z, Jayawant S. A novel ARX phenotype: rapid neurodegeneration with Ohtahara syndrome and a dyskinetic movement disorder. *Dev Med Child Neurol*. 2009;3:305–307.
8. Kato M, Koyama N, Ohta M, Miura K, Hayasaka K. Frameshift mutations of the ARX gene in familial Ohtahara syndrome. *Epilepsia*. 2010;51:1679–1684.
9. Saitsu H, Kato M, Mizuguchi T, Hamada K, Osaka H, Tohyama J, Uruno K, Kumada S, Nishiyama K, Nishimura A, Okada I, Yoshimura Y, Hirai S, Kumada T, Hayasaka K, Fukuda A, Ogata K, Matsumoto N. De novo mutations in the gene encoding STXBP1 (MUNC18-1) cause early infantile epileptic encephalopathy. *Nat Genet*. 2008;40:782–788.
10. Engel J Jr. Report of the ILAE classification core group. *Epilepsia*. 2006;47:1558–1568.
11. Molinari F, Raas-Rothschild A, Rio M, Fiermonte G, Encha-Razavi F, Palmieri L, Palmieri F, Ben-Neriah Z, Kadhom N, Vekemans M, Attie-Bitach T, Munnich A, Rustin P, Colleaux L. Impaired mitochondrial glutamate transport in autosomal recessive neonatal myoclonic epilepsy. *Am J Hum Genet*. 2005;76:334–339.
12. Molinari F, Kaminska A, Fiermonte G, Boddaert N, Raas-Rothschild A, Plouin P, Palmieri L, Brunelle F, Palmieri F, Dulac O, Munnich A, Colleaux L. Mutations in the mitochondrial glutamate carrier SLC25A22 in neonatal epileptic encephalopathy with suppression bursts. *Clin Genet*. 2009;76:188–194.
13. Kato M, Das S, Petras K, Sawaishi Y, Dobyns WB. Polyalanine expansion of ARX associated with cryptogenic West syndrome. *Neurology*. 2003;61:267–268.
14. Guerrini R, Moro F, Kato M, Barkovich AJ, Shiihara T, McShane MA, Hurst J, Loi M, Tohyama J, Norci V, Hayasaka K, Kang UJ, Das S, Dobyns WB. Expansion of the first PolyA tract of ARX causes infantile spasms and status dystonicus. *Neurology*. 2007;69:427–433.
15. Stromme P, Mangelsdorf ME, Shaw MA, Lower KM, Lewis SM, Bruyere H, Lutcherath V, Gedeon AK, Wallace RH, Scheffer IE, Turner G, Partington M, Frints SG, Fryns JP, Sutherland GR, Mulley JC, Gecz J. Mutations in the human ortholog of Aristaless cause X-linked mental retardation and epilepsy. *Nat Genet*. 2002;30:441–445.
16. Verhage M, Maia AS, Plomp JJ, Brussaard AB, Heeroma JH, Vermeer H, Toonen RF, Hammer RE, van den Berg TK, Missler M, Geuze HJ, Sudhof TC. Synaptic assembly of the brain in the absence of neurotransmitter secretion. *Science*. 2000;287:864–869.
17. Garcia EP, Gatti E, Butler M, Burton J, De Camilli P. A rat brain Sec1 homologue related to Rop and UNC18 interacts with syntaxin. *Proc Natl Acad Sci USA*. 1994;91:2003–2007.
18. Kalidas S, Santosh V, Shareef MM, Shankar SK, Christopher R, Shetty KT. Expression of p67 (Munc-18) in adult human brain and neuroectodermal tumors of human central nervous system. *Acta Neuropathol*. 2000;99:191–198.
19. Saitsu H, Kato M, Okada I, Kenji O, Higuchi T, Hoshino H, Kubota M, Arai H, Kimura S, Sudo A, Miyama S, Takami Y, Watanabe T, Nishimura A, Nishiyama K, Miyake N, Wada T, Osaka H, Kondo N, Hayasaka K, Matsumoto N. *STXBP1* mutations in early infantile epileptic encephalopathy with suppression-burst pattern. *Epilepsia*. 2010;51:2397–2405.
20. Kanazawa K, Kumada S, Kato M, Saitsu H, Kurihara E, Matsumoto N. Choreo-ballistic movements in a case carrying a missense mutation in syntaxin binding protein 1 gene. *Mov Disord*. 2010;25:2265–2267.
21. Dulubova I, Khvotchev M, Liu S, Huryeva I, Sudhof TC, Rizo J. Munc18-1 binds directly to the neuronal SNARE complex. *Proc Natl Acad Sci USA*. 2007;104:2697–2702.
22. Toonen RF, Verhage M. Munc18-1 in secretion: lonely Munc joins SNARE team and takes control. *Trends Neurosci*. 2007;30:564–572.
23. Rickman C, Medine CN, Bergmann A, Duncan RR. Functionally and spatially distinct modes of munc18-syntaxin 1 interaction. *J Biol Chem*. 2007;282:12097–12103.
24. Shyu AB, Wilkinson MF, van Hoof A. Messenger RNA regulation: to translate or to degrade. *EMBO J*. 2008;27:471–481.
25. Maquat LE, Kinniburgh AJ, Rachmilewitz EA, Ross J. Unstable beta-globin mRNA in mRNA-deficient β° thalassemia. Cell. 1981;27:543–553.
26. Sudhof TC. The synaptic vesicle cycle. *Annu Rev Neurosci*. 2004;27:509–547.
27. Weimer RM, Richmond JE. Synaptic vesicle docking: a putative role for the Munc18/Sec1 protein family. *Curr Top Dev Biol*. 2005;65:83–113.
28. Rizo J, Rosenmund C. Synaptic vesicle fusion. *Nat Struct Mol Biol*. 2008;15:665–674.
29. Gurnett CA, Hedera P. New ideas in epilepsy genetics: novel epilepsy genes, copy number alterations, and gene regulation. *Arch Neurol*. 2007;64:324–328.
30. Garcia CC, Blair HJ, Seager M, Coulthard A, Tennant S, Buddles M, Curtis A, Goodship JA. Identification of a mutation in synapsin I, a synaptic vesicle protein, in a family with epilepsy. *J Med Genet*. 2004;41:183–186.
31. Toonen RF, Wierda K, Sons MS, de Wit H, Cornelisse LN, Brussaard A, Plomp JJ, Verhage M. Munc18-1 expression levels control synapse recovery by regulating readily releasable pool size. *Proc Natl Acad Sci USA*. 2006;103:18332–18337.
32. Kitamura K, Yanazawa M, Sugiyama N, Miura H, Iizuka-Kogo A, Kusaka M, Omichi K, Suzuki R, Kato-Fukui Y, Kamiirisa K, Matsuo M, Kamijo S, Kasahara M, Yoshioka H, Ogata T, Fukuda T, Kondo I, Kato M, Dobyns WB, Yokoyama M, Morohashi K. Mutation of ARX causes abnormal development of forebrain and testes in mice and X-linked lissencephaly with abnormal genitalia in humans. *Nat Genet*. 2002;32:359–369.
33. Bonneau D, Toutain A, Laquerriere A, Marret S, Saugier-Veber P, Barthez MA, Radi S, Biran-Mucignat V, Rodriguez D, Gelot A. X-linked lissencephaly with absent corpus callosum and ambiguous genitalia (XLAG): clinical, magnetic resonance imaging, and neuropathological findings. *Ann Neurol*. 2002;51:340–349.
34. Kato M. A new paradigm for West syndrome based on molecular and cell biology. *Epilepsy Res*. 2006;70(suppl 1):S87–S95.
35. Kato M, Dobyns WB. X-linked lissencephaly with abnormal genitalia as a tangential migration disorder causing intractable epilepsy: proposal for

a new term, "interneuronopathy." *J Child Neurol.* 2005;20:392–397.
36. Hamdan FF, Piton A, Gauthier J, Lortie A, Dubeau F, Dobrzeniecka S, Spiegelman D, Noreau A, Pellerin S, Cote M, Henrion E, Fombonne E, Mottron L, Marineau C, Drapeau P, Lafreniere RG, Lacaille JC, Rouleau GA, Michaud JL. De novo STXBP1 mutations in mental retardation and nonsyndromic epilepsy. *Ann Neurol.* 2009;65:748–753.
37. Guilmatre A, Dubourg C, Mosca AL, Legallic S, Goldenberg A, Drouin-Garraud V, Layet V, Rosier A, Briault S, Bonnet-Brilhault F, Laumonnier F, Odent S, Le Vacon G, Joly-Helas G, David V, Bendavid C, Pinoit JM, Henry C, Impallomeni C, Germano E, Tortorella G, Di Rosa G, Barthelemy C, Andres C, Faivre L, Frebourg T, Saugier Veber P, Campion D. Recurrent rearrangements in synaptic and neurodevelopmental genes and shared biologic pathways in schizophrenia, autism, and mental retardation. *Arch Gen Psychiatry.* 2009;66:947–956.
38. Ramocki MB, Zoghbi HY. Failure of neuronal homeostasis results in common neuropsychiatric phenotypes. *Nature.* 2008;455:912–918.

Chapter 65

mTOR and Epileptogenesis in Developmental Brain Malformations

Michael Wong
Peter B. Crino

INTRODUCTION

Malformations of cortical development (MCDs) are among the most common causes of epilepsy. While a wide variety of types and classifications of MCDs exists,[1] a subset of focal cortical malformations (FCMs), including tuberous sclerosis complex (TSC), focal cortical dysplasia, ganglioglioma, and hemimegalencephaly, is associated with an especially high incidence of epilepsy and other neurological deficits, such as cognitive dysfunction and autism.[2,3] Epilepsy related to these focal developmental brain malformations is often refractory to medical therapy. Even in patients whose seizures are well controlled with medications, currently available drugs are only symptomatic treatments that help suppress seizures; they have not been demonstrated to have antiepileptogenic or disease-modifying properties in preventing or altering the long-term prognosis of epilepsy. Although epilepsy surgery may eliminate seizures in some medically intractable cases, many patients are not good candidates for surgery or continue to have seizures despite surgical intervention. Thus, novel therapeutic strategies are needed to reduce the burden of seizures and other neurological symptoms caused by MCDs or, ideally, to prevent the development of epilepsy in the first place.

Tuberous sclerosis complex (TSC) is often viewed as a prototypical FCM associated with epilepsy, providing a detailed understanding of the clinical features, the pathological substrates, and now the molecular-genetic pathophysiology of this disease.[4,5] Up to 90% of patients with TSC have epilepsy, most of whom are refractory to seizure medications.[6] The cortical tuber is the pathological hallmark of TSC and is strongly correlated with the neurological manifestations, including seizures, cognitive disability, and autism. Cortical tubers are characterized by a focal loss of normal cortical organization or lamination and the presence of a spectrum of abnormal dysmorphic or cytomegalic cell types. Although the mechanisms causing epilepsy in TSC are incompletely understood, a number of cellular and molecular abnormalities have been identified in both tuber and peri-tuber tissue from TSC patients that likely promote epileptogenesis and other neurological deficits in TSC, such as molecular

Dominant-Negative Mutations in α-II Spectrin Cause West Syndrome with Severe Cerebral Hypomyelination, Spastic Quadriplegia, and Developmental Delay

Hirotomo Saitsu,[1,*] Jun Tohyama,[2] Tatsuro Kumada,[3] Kiyoshi Egawa,[3] Keisuke Hamada,[4] Ippei Okada,[1] Takeshi Mizuguchi,[1,17] Hitoshi Osaka,[5] Rie Miyata,[6] Tomonori Furukawa,[3] Kazuhiro Haginoya,[7] Hideki Hoshino,[8] Tomohide Goto,[9] Yasuo Hachiya,[10] Takanori Yamagata,[11] Shinji Saitoh,[12] Toshiro Nagai,[13] Kiyomi Nishiyama,[1] Akira Nishimura,[1] Noriko Miyake,[1] Masayuki Komada,[14] Kenji Hayashi,[15] Syu-ichi Hirai,[15] Kazuhiro Ogata,[4] Mitsuhiro Kato,[16] Atsuo Fukuda,[3] and Naomichi Matsumoto[1,*]

A de novo 9q33.3-q34.11 microdeletion involving *STXBP1* has been found in one of four individuals (group A) with early-onset West syndrome, severe hypomyelination, poor visual attention, and developmental delay. Although haploinsufficiency of *STXBP1* was involved in early infantile epileptic encephalopathy in a previous different cohort study (group B), no mutations of *STXBP1* were found in two of the remaining three subjects of group A (one was unavailable). We assumed that another gene within the deletion might contribute to the phenotype of group A. *SPTAN1* encoding α-II spectrin, which is essential for proper myelination in zebrafish, turned out to be deleted. In two subjects, an in-frame 3 bp deletion and a 6 bp duplication in *SPTAN1* were found at the initial nucleation site of the α/β spectrin heterodimer. *SPTAN1* was further screened in six unrelated individuals with WS and hypomyelination, but no mutations were found. Recombinant mutant (mut) and wild-type (WT) α-II spectrin could assemble heterodimers with β-II spectrin, but α-II (mut)/β-II spectrin heterodimers were thermolabile compared with the α-II (WT)/β-II heterodimers. Transient expression in mouse cortical neurons revealed aggregation of α-II (mut)/β-II and α-II (mut)/β-III spectrin heterodimers, which was also observed in lymphoblastoid cells from two subjects with in-frame mutations. Clustering of ankyrinG and voltage-gated sodium channels at axon initial segment (AIS) was disturbed in relation to the aggregates, together with an elevated action potential threshold. These findings suggest that pathological aggregation of α/β spectrin heterodimers and abnormal AIS integrity resulting from *SPTAN1* mutations were involved in pathogenesis of infantile epilepsy.

Introduction

West syndrome (WS) is a common infantile epileptic syndrome characterized by brief tonic spasms, an electroencephalogram pattern called hypsarrhythmia, and mental retardation.[1] Brain malformations and metabolic disorders can be underlying causes of WS, but many cases remain etiologically unexplained.[1] Only two causative genes, *ARX* (MIM *300382) and *CDKL5* (MIM *300203), are mutated in a subset of familial and sporadic X-linked WS cases (ISSX1 and ISSX2 [MIM #308350 and #300672]).[2–4] Early infantile epileptic encephalopathy with suppression-burst (EIEE) is the earliest form of infantile epileptic syndrome.[5,6] The transition from EIEE to WS occurs in 75% of individuals with EIEE, suggesting a common pathological mechanism between these two syndromes.[5,6] We have recently reported that de novo mutations of *STXBP1* (MIM *602926) cause EIEE.[7]

Spectrins are submembranous scaffolding proteins involved in the stabilization of membrane proteins.[8,9] Spectrins are flexible and long molecules consisting of α and β subunits, which are assembled in an antiparallel side-by-side manner into heterodimers. Heterodimers form by end-to-end tetramers integrating into the membrane cytoskelton.[8,9] The spectrin repertoire in humans includes two α subunits and five β subunits. Defects of erythroid α-I and β-I spectrins and neuronal β-III spectrin are associated with hereditary spherocytosis (SPH3 and SPH2 [MIM

[1]Department of Human Genetics, Yokohama City University Graduate School of Medicine, 3-9 Fukuura, Kanazawa-ku, Yokohama 236-0004, Japan; [2]Department of Pediatrics, Epilepsy Center, Nishi-Niigata Chuo National Hospital, 1-14-1 Masago, Nishi-ku, Niigata 950-2085, Japan; [3]Department of Physiology, Hamamatsu University School of Medicine, 1-20-1 Handayama, Hamamatsu 431-3192, Japan; [4]Department of Biochemistry, Yokohama City University Graduate School of Medicine, 3-9 Fukuura, Kanazawa-ku, Yokohama 236-0004, Japan; [5]Division of Neurology, Clinical Research Institute, Kanagawa Children's Medical Center, 2-138-4 Mutsukawa, Minami-ku, Yokohama 232-8555, Japan; [6]Department of Pediatrics, Tokyo Kita Shakai Hoken Hospital, 4-17-56 Akabanedai, Kita-ku, Tokyo 115-0053, Japan; [7]Department of Pediatrics, Tohoku University School of Medicine, 1-1 Seiryo-machi, Aoba-ku, Sendai 980-8574, Japan; [8]Division of Neurology, National Center for Child Health and Development, 2-10-1 Okura, Setagaya-ku, Tokyo 157-8535, Japan; [9]Department of Neurology, Tokyo Metropolitan Children's Medical Center, 2-8-29 Musashidai, Fuchu 183-8561, Japan; [10]Department of Neuropediatrics, Tokyo Metropolitan Neurological Hospital, 2-6-1 Musashidai, Fuchu 183-0042, Japan; [11]Department of Pediatrics, Jichi Medical University, 3311-1 Yakushiji, Shimotsuke, Tochigi 329-0498, Japan; [12]Department of Pediatrics, Hokkaido University Graduate School of Medicine, North 15, West 7, Kita-ku, Sapporo 060-8638, Japan; [13]Department of Pediatrics, Dokkyo Medical University, Koshigaya Hospital, 2-1-50 Minami-Koshigaya, Koshigaya, Saitama 343-8555, Japan; [14]Department of Biological Sciences, Faculty of Bioscience and Biotechnology, Tokyo Institute of Technology, 4259-B-16 Nagatsuta, Midori-ku, Yokohama 226-8501, Japan; [15]Department of Molecular Biology, Yokohama City University Graduate School of Medicine, 3-9 Fukuura, Kanazawa-ku, Yokohama 236-0004, Japan; [16]Department of Pediatrics, Yamagata University School of Medicine, 2-2-2 Iida-nishi, Yamagata 990-9585, Japan
[17]Present address: Laboratory of Biochemistry and Molecular Biology, National Cancer Institute, National Institutes of Health, Building 37, Room 6050, Bethesda, MD 20892, USA
*Correspondence: hsaitsu@yokohama-cu.ac.jp (H.S.), naomat@yokohama-cu.ac.jp (N.M.)
DOI 10.1016/j.ajhg.2010.04.013.

#270970 and +182870]) and spinocerebellar ataxia type 5 (SCA5 [MIM #600224]), respectively.[8,10,11] The α-II spectrin is considered as the major α spectrin expressed in nonerythroid cells, and α-II/β-II spectrin heterodimers are the predominant species in these cells.[9,12] Abnormal development of nodes of Ranvier and destabilizing initial clusters of voltage-gated sodium channels (VGSC) were observed in zebrafish α-II spectrin mutants harboring a nonsense mutation. The mutants also showed impaired myelination in motor nerves and in the dorsal spinal cord, suggesting that α-II spectrin plays important roles in the maintenance of the integrity of myelinated axons.[13]

Here, we describe three cases of early-onset WS with cerebral hypomyelination harboring *SPTAN1* (MIM *182810) aberrations. Two individuals with in-frame mutations showed more severe phenotypes than one individual with *SPTAN1* and *STXBP1* deletion. In-frame mutations of *SPTAN1* result in aggregation of α-II (mut)/β-II and α-II (mut)/β-III spectrin heterodimers, suggesting dominant-negative effects of the mutations. Spectrin aggregation is associated with disturbed clustering of VGSC and an elevated action potential threshold. Our findings revealed essential roles of α-II spectrin in human brain development and suggest that abnormal AIS is possibly involved in pathogenesis of infantile epilepsy.

Subjects and Methods

Subjects

Subjects 1, 2, and 3 have been originally reported as three of four individuals with early onset WS, severe hypomyelination, reduced white matter, and developmental delay (group A: subjects 1, 2, and 3 were previously named as No. 2, No. 1, and No. 3, respectively, and No. 4 was unavailable for this study).[14] Subject 1 has been shown to possess a 9q33.3-q34.11 microdeletion including *STXBP1*.[7] Clinical information of these three subjects with *SPTAN1* aberrations is updated in Table S1 available online. We screened for *SPTAN1* mutations in a total of eight unrelated individuals with WS accompanied by severe hypomyelination without episodes of prenatal incidents or neonatal asphyxia (six males and two females, including subjects 2 and 3 of group A). Individuals with these two distinctive features (WS and severe hypomyelination) are relatively rare. These eight patients were totally different from the previously investigated 13 EIEE patients (group B).[7] Screening tests for metabolic disorders (lactate, amino acids, and uric organic acids) were normal in all subjects. *ARX* and *CDKL5* were not mutated in the six male and two female patients, respectively. The diagnosis was made on the basis of clinical features, including tonic spasms with clustering, arrest of psychomotor development, and hypsarrhythmia on electroencephalogram, as well as brain magnetic resonance imaging (MRI) findings. Experimental protocols were approved by the Committee for Ethical Issues at Yokohama City University School of Medicine. Informed consent was obtained from all individuals included in this study, in agreement with the requirements of Japanese regulations.

Mutation Analysis

Genomic DNA was obtained from peripheral blood leukocytes by standard methods, amplified by GenomiPhi version 2 (GE Healthcare, Buckinghamshire, UK), and used for mutational screening. Exons 2 to 57, covering the *SPTAN1* coding region (of transcript variant 1, GenBank accession number NM_001130438), were screened by high-resolution melting curve (HRM) analysis as previously described.[7] In transcript variant 2 (GenBank accession number NM_003127), the only difference is that exon 37 of variant 1 was missing. PCR conditions and primer sequences are shown in Table S2. If a sample showed an aberrant melting curve shift, the PCR product was sequenced. All mutations were also verified on PCR products directly via genomic DNA (not amplified by GenomiPhi) as a template. DNAs from 250 Japanese normal controls were screened for the two in-frame *SPTAN1* mutations by HRM analysis. Normal controls which showed aberrant melting curve shift were sequenced.

Parentage Testing

For all families showing de novo mutations, parentage was confirmed by microsatellite analysis as previously described.[7] Biological parentage was judged if more than four informative markers were compatible and other uninformative markers showed no discrepancies.

Expression Vectors

A full-length human *SPTAN1* cDNA was prepared by PCR with first-strand cDNA derived from a human lymphoblastoid cells (LCL) and an IMAGE clone (clone ID 5211391) as a template. The obtained *SPTAN1* cDNA was sequenced and confirmed to be identical to a RefSeq mRNA (amino acids 1–2477, GenBank accession number NM_001130438) except for two synonymous base substitutions that have been registered in dbSNP as rs2227864 and rs2227862. Site-directed mutagenesis via a KOD-Plus-Mutagenesis kit (Toyobo, Osaka, Japan) was used to generate *SPTAN1* mutants including c.6619_6621 del (p.E2207 del) and c.6923_6928 dup (p.R2308_M2309 dup). A C-terminal Flag-tag was introduced by PCR. All variant cDNAs were verified by sequencing. C-terminal Flag-tagged WT and mutant *SPTAN1* cDNAs were cloned into the pCIG vector[15,16] to express C-terminal Flag-tagged α-II spectrin as well as nuclear-localized EGFP. WT and mutant *SPTAN1* cDNAs were also cloned into the pCAG-EGFP-C1 vector, in which EGFP gene and multiple cloning sites of pEGFP-C1 vector (Clontech, Mountain View, CA) are introduced into a CAG-promoter vector,[15,16] to express N-terminal EGFP-tagged α-II spectrin.

For protein expression in *Escherichia coli*, WT and mutant *SPTAN1* cDNAs (amino acids 1445–2477, the last eight spectrin repeats and the EF hand domain) were cloned into pGEX6P-3 (GE Healthcare) to generate glutathione S-transferase (GST) fusion proteins. Human *SPTBN1* cDNAs (amino acids 1–1139, GenBank accession number NM_003128, including the actin binding domain and eight spectrin repeats) were prepared by PCR via first-strand cDNA derived from a human LCL, and were cloned into pET-24a (Merck, Darmstadt, Germany) to generate His-tag fusion proteins.

Protein Expression, Purification, and Binding Assay

Proteins were expressed in *Escherichia coli* BL21 (DE3). Bacteria were grown at 37°C in Lysogeny Broth media with 300 μg/ml ampicillin to a density yielding an absorbance at 600 nm of 0.8. Protein expression was then induced with 1 mM isopropyl-β-D-thiogalactoside (IPTG) at 20°C overnight. Cells were collected by centrifugation and lysed by sonication. Proteins were purified by

affinity chromatography with Glutathione Sepharose High Performance (GE Healthcare) for GST-α-II spectrin or HisTrap HP (GE Healthcare) for β-II spectrin-His. α-II spectrins were further purified by HiTrap Q HP (GE Healthcare) and Superdex-200 (GE Healthcare) columns in a buffer containing 150 mM NaCl, 20 mM sodium phosphate buffer (pH 7.5), and 2 mM dithiothreitol (DTT). β-II spectrin was further purified by Superdex-200 (GE Healthcare) columns in a buffer containing 1 M NaCl, 20 mM sodium phosphate buffer (pH 7.5), and 2 mM DTT.

For the GST pull-down assay to examine the assembly of α-II/β-II heterodimers, 0.5 μM GST-α-II spectrin (WT, del mut, or dup mut) or 1 μM GST were preincubated with 1 μM β-II spectrin-His for 1 hr at 4°C with gentle agitation in binding buffer containing 150 mM NaCl, 20 mM sodium phosphate buffer (pH 7.5), and 2 mM DTT. The reaction mixture (100 μl) was transferred onto an Ultrafree-MC (Millipore, Billerica, MA), containing 50 μl of a 75% slurry of Glutathione Sepharose 4B equilibrated in binding buffer, and incubated overnight at 4°C. Unbound proteins were recovered by centrifugation at 500 × g for 2 min. The beads were washed three times with the binding buffer. The bound molecules were eluted with a buffer containing 100 mM NaCl, 20 mM sodium phosphate buffer (pH 7.5), 5 mM DTT, 1 mM EDTA, and 50 mM reduced glutathione. The eluted fractions were analyzed by SDS-PAGE, and protein bands were visualized by staining with Coomassie brilliant blue. For the analytical gel filtration experiments, 3.3 μM GST-α-II spectrin (WT, del mut, or dup mut) were preincubated with or without 3.3 μM β-II spectrin-His for 3 hr at 4°C with gentle agitation in a binding buffer containing 150 mM NaCl, 20 mM sodium phosphate buffer (pH 7.5), and 2 mM DTT. The samples were analyzed by Superdex-200 column equilibrated in binding buffer. The eluted fractions were analyzed by SDS-PAGE and protein bands were visualized by staining with Coomassie brilliant blue.

Structural Prediction

The structure of human α-II spectrin was predicted by homology modeling with Phyre,[17] based on sequence homology between human α-II spectrin (1981–2315 aa) and chicken brain alpha spectrin (1662–1982 aa) (Protein data bank ID, 1U4Q).[18] The structure and positions of mutations were illustrated by PyMOL with the crystal structure of 1U4Q.

Circular Dichroism Measurements

For circular dichroism (CD) measurements, GST-α-II spectrin were digested with human rhinovirus 3C protease at 4°C, and then the GST-tag was removed by affinity chromatography with glutathione sepharose 4B (GE Healthcare). We measured far-UV CD spectra and estimated the secondary structure as previously described.[7] In brief, the experiments were performed in 20 mM sodium phosphate buffer (pH 7.5) containing 150 mM NaCl, 2 mM DTT with or without 1 mM $CaCl_2$, which stabilizes the structure of the EF hand domain. α-II and β-II spectrin concentration was adjusted to 1.7 μM (without $CaCl_2$) and 1.5 μM (with $CaCl_2$). Melting (transition midpoint) temperature (T_m) was calculated by fitting a sigmoid-function equation with KaleidaGraph (Synergy Software, Reading, PA). The data from three independent experiments were averaged and the SD was calculated. Similar results were obtained in the presence or absence of 1 mM $CaCl_2$.

Cell Culture, Transfection, and Immunofluorescence

For primary neuronal cultures for immunofluorescence, cortexes dissected from mice (embryonic days 14 to 15) were dissociated in 0.05% trypsin-EDTA solution (Invitrogen, Carlsbad, CA), and triturated with a Pasteur pipette. The dissociated cells were plated on 200 μg/ml poly-D-lysine (Millipore)/20 μg/ml laminin (Invitrogen)-coated glass coverslips at a density of 15,000 cells/cm^2. Expression vectors were introduced at the time of dissociation by electroporation, with the Amaxa Mouse Neuron Nucleofector kit (Lonza, Tokyo, Japan) according to the manufacturer's protocol (Program O-005), and 2 μg plasmid DNA per condition. After cortical neurons attached to coverslips, the medium was changed from normal medium (10% FBS in DMEM) to maintaining medium (2% B27 and 1 × penicillin-streptomycin-glutamine in Neurobasal [Invitrogen]). Half of the medium was replaced with an equal volume of maintaining medium every 4 days. LCLs were grown in RPMI 1640 medium supplemented with 10% FBS, 1 × antibiotic-antimycotic (Invitrogen), and 8 μg/ml tylosin (Sigma, Tokyo, Japan) at 37°C in a 5% CO_2 incubator. For the immunofluorescence imaging study, LCLs were plated on coated coverslips as described above for 3–6 hr.

Neurons and LCLs were fixed with 2% paraformaldehyde in PBS for 15 min and permeabilized with 0.1% Triton X-100 for 5 min. For detection of VGSCs, cells were fixed with methanol at −20°C for 10 min. Cells were then blocked with 10% normal goat serum for 30 min. Primary antibodies used for the study were shown in figure legends. Secondary antibodies, highly purified to minimize cross-reactivity, were used: Alexa-488-conjugated goat anti-mouse, anti-rabbit, and anti-chicken (Invitrogen), and Cy3-conjugated goat anti-mouse, anti-rabbit, and anti-chicken (Jackson ImmunoResearch, West Grove, PA). Coverslips were mounted with Vectashield (Vector Laboratories, Burlingame, CA) that contained 4,6-diamidino-2-phenylindole (DAPI) and visualized with an AxioCam MR CCD fitted to Axioplan2 fluorescence microscope (Carl Zeiss, Oberkochen, Germany). We captured images with Axio Vision 4.6 software (Carl Zeiss). Immunofluorescence of aggregated mutant α/β spectrins was much brighter than WT α/β spectrins, leading to constant short exposure time compared with the WT. For detection of ankyrinG and VGSCs, the exposure time was fixed in a series of experiments in order to enable direct comparison between different samples. For evaluation of ankyrinG and VGSC expression, 50 isolated transfected neurons were analyzed in each experiment, and representative cells were photographed. The results were confirmed at least in three independent experiments.

Electrophysiology

Mouse neocortices at embryonic day 15 were dissociated and plated on poly-L-lysine-coated plastic coverslips (Cell desk LF, MS-0113L; Sumitomo Bakelite, Tokyo, Japan) at a density of about 100,000 cells/cm^2. 1 μg of expression vector for either WT, del mut, or dup mut α-II spectrin was introduced at the time of dissociation by electroporation with an Amaxa Mouse Neuron Nucleofector kit (Lonza). Primary cortical neurons were cultured in neurobasal medium supplemented with B27 and penicillin-streptomycin-glutamine (Invitrogen). During the culture period, one-half of the medium was changed every day. Whole-cell patch-clamp recordings were obtained from mice neocortical neurons at 9 days in vitro (DIV) neuronal culture. A coverslip was assembled to recording chambers on the stages of upright microscopes (Olympus, Tokyo, Japan) and continuously perfused with oxygenated, standard artificial cerebrospinal fluid (ACSF) at a flow rate of 2 ml/min and a temperature of 30°C. The standard ACSF solution contained the following (mM): 126 NaCl, 2.5 KCl,

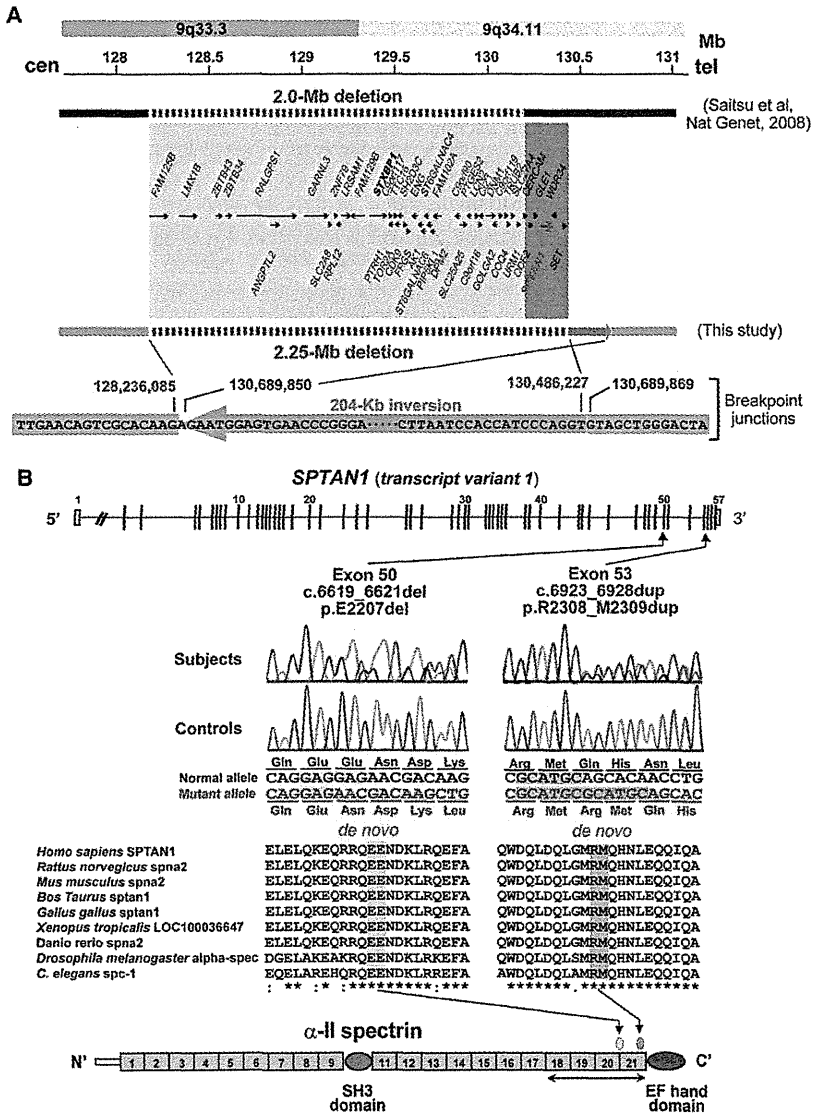

Figure 1. *SPTAN1* Aberrations in Individuals with West Syndrome and Cerebral Hypomyelination

(A) Genomic rearrangements at 9q33.3-q34.11 in subject 1. Top depicts chromosomal bands and genomic location (Mb) from the p telomere (cen, toward the centromere; tel, toward the telomere). Our previous study by BAC array could reveal the approximate size of the deletion (2.0 Mb) (horizontal line above boxes).[7] The deletion was newly analyzed by Affymetrix GeneChip 250K array and turned out to be 2.25 Mb in size (chr9:128,236,086-130,486,226) (UCSC genome browser coordinate [version Mar. 2006]) (horizontal line below boxes). Blue and red boxes indicate old and renewed deletion intervals, respectively. Five RefSeq genes (*ODF2*, *GLE1*, *SPTAN1*, *WDR34*, and *SET*) were newly found (in red box). The rearrangements include an unexpected 204 kb inversion (green arrow). Intact genomic regions are shown in sky blue.

(B) Schematic representation of *SPTAN1* (transcript variant 1) consisting of 57 exons (UTR and coding region are open and filled rectangles, respectively). Exon 37 of transcript variant 1 is missing in variant 2, the only difference between the two transcripts. Two distinct mutations were found at evolutionary conserved amino acids in triple helical repeats (spectrin repeats). All these mutations occured de novo. Homologous sequences were aligned with the CLUSTALW web site. α-II spectrin consists of 22 domains (numbered), including 20 spectrin repeats, an SH3 domain, and an EF hand domain. The mutations occurred within the last four spectrin repeats, which are required for α/β heterodimer association (bidirectional arrow).

1.25 NaH_2PO_4, 2.0 $MgSO_4$, 2.0 $CaCl_2$, 26.0 $NaHCO_3$, and 20.0 glucose. The images of cells were acquired with Olympus BX51 or BX61 microscopes equipped with electron-multiplying CCD (EMCCD) cameras, #C9100-13 or #C9100-02 (Hamamatsu Photonics, Hamamatsu, Japan), respectively. Transfected cells were selected for recordings by their fluorescence in the nucleus via a 40× water-immersion objective lens (UMPlanFI, Olympus). Membrane currents and membrane potentials were recorded with an Axopatch 700A and 200B amplifier, respectively. Signals were low-pass filtered at 10 kHz and digitized at 50 kHz by means of Digidata 1332A data-acquisition system (Molecular Devices, Tokyo, Japan). Passive membrane properties and action potentials were recorded with patch pipettes (5.8–8.0 MΩ) filled with the following intercellular solutions (in mM): 130 K-methanesulfonic acid, 10 KCl, 2 $MgCl_2$, 0.1 EGTA, and 10 HEPES (pH 7.3) with KOH. For current clamp experiments, cells were held at −60 mV by constant current injection as needed, and their firing pattern were recorded in response to sustained depolarizing current injections (500 ms duration, +10 pA increments) to analyze the input-output relationship in each cell. A single action potential was also evoked to determine their firing threshold. The injection current amplitude (10 ms duration) was increased in 2–10 pA increments from a subthreshold to an intensity well beyond threshold. Voltage-clamp studies for sodium currents were carried out with patch pipettes (5.8–8.0 MΩ) filled with the following intercellular solutions (mM): 145 tetraethylammonium-Cl, 15 NaCl, 2 $MgCl_2$, 10 EGTA, 10 HEPES, 3 MgATP, and 0.4 GTP (pH 7.4) with NaOH. Series resistance was usually below 20 MΩ and compensated by 70%–80%. The remaining linear capacitive and leakage currents were subtracted off-line by scaling average traces recorded at hyperpolarized voltages. Voltage-dependent inward sodium currents were elicited by 500 ms depolarizing steps in 5 mV increments from −90 to +10 mV at a holding membrane potential of −90 mV. For measuring the inactivation protocol of sodium currents, 500 ms long prepotentials started at − 90 mV and were incremented by 5 mV steps while the command potential was kept constant at −30 mV. The current elicited during each test pulse was normalized to the maximal current (I/Imax). Statistical

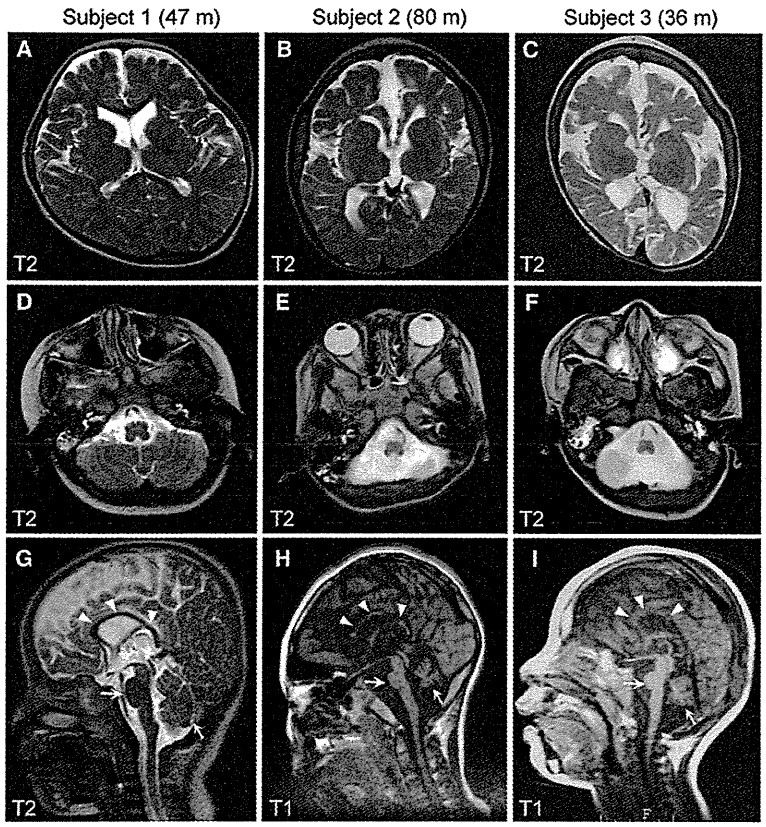

Figure 2. Brain MRI of Subjects with *SPTAN1* Aberrations at the Most Recent Developmental Stages

(A–C) T2-weighted axial images through the basal ganglia. Subject 1 (with a 2.25 Mb deletion) showed only slightly reduced white matter (A). By contrast, cortical atrophy and severe hypomyelination with strikingly reduced volume of white matter were evident, especially in the frontal lobes, in subjects with in-frame mutations (subjects 2 and 3) (B and C).

(D–I) T2-weighted axial images through the brainstem/cerebellum (D–F) and T2- (G) or T1-weighted midline sagittal images (H and I). Compared with subject 1 (D and G), subjects 2 (E and H) and 3 (F and I) show a thinned and shortened corpus callosum (arrowheads), severe atrophy of the brainstem, and hypoplasia and/or atrophy of the cerebellar hemispheres and vermis (arrows). m, months.

analyses were made with two-way repeated-measures ANOVA followed by a Bonferroni post-test for analysis of the input-output relationship and current amplitude at every voltage step. One-way ANOVA followed by Dunnet's posthoc test was applied for threshold, peak current, kinetics of action potentials, and passive membrane properties. The results are given as mean ± SEM, and threshold p value for statistical significance was 0.05. Statistical comparisons were performed with the Prism 4.0 (GraphPad software, La Jolla, CA).

Results

Identification of *SPTAN1* In-Frame Mutations

We previously reported a de novo 9q33.3-q34.11 microdeletion involving *STXBP1* in an individual with EIEE, who transited afterward to WS at the age of 3 months (subject 1).[7] Subject 1 was originally reported as one of four individuals (group A) who showed early onset WS and severe cerebral hypomyelination (as patient No. 2).[14] It is likely that haploinsufficiency of *STXBP1* caused EIEE and subsequent WS in subject 1;[7] however, no mutations of *STXBP1* were found in two of the remaining three individuals of group A (subjects 2 and 3, previously described as No. 1 and No. 3, and No. 4 was unavailable for this study).[14] Based on obvious severe hypomyelination of the group A individuals, we hypothesized that another gene within the deletion may contribute to the phenotype of group A, especially for severe hypomyelination. Re-examination of the deletion interval by genomic microarray and long PCR successfully determined the 2.25 Mb deletion and the associated 204 kb inversion (Figure 1A and see Figure S1). Among the 46 genes mapped within the deletion, *SPTAN1*, which encodes α-II spectrin, appeared to be a primary candidate because zebrafish α-II spectrin mutants showed impaired myelination.[13] We found de novo heterozygous mutations in *SPTAN1* in subjects 2 and 3 (parentage was confirmed in their respective families). Subject 2 has an in-frame 3-bp deletion (c.6619_6621 del) leading to p.E2207 del in the continuous helix region between the last two spectrin repeats, and subject 3 has an in-frame 6 bp duplication (c.6923_6928 dup, p.R2308_M2309 dup) within the last spectrin repeat (Figure 1B). These two mutations were absent in 250 Japanese normal controls (500 alleles). *SPTAN1* was further screened in six unrelated individuals with WS and hypomyelination similar to the phenotype of group A (not belonging to group B), but no mutations were found.

Phenotypes Associated with *SPTAN1* Aberrations

The clinical features of the three subjects with *SPTAN1* aberrations are summarized in Table S1. Subjects 2 and 3 showed severe spastic quadriplegia, no developmental progress, and poor visual attention. Epileptic seizures were resistant to various treatments. Subject 3 died of fulminant myocarditis at 3 years of age. In contrast, subject 1 showed slight psychomotor development with eye contact, but no head control. Her seizures have been well controlled. Brain MRI of subjects 2 and 3 revealed widespread brain atrophy including brainstem, hypoplasia, and/or atrophy of the cerebellar hemispheres and vermis, ventriculomegaly, a thinned and shortened corpus callosum, and severe hypomyelination with strikingly reduced white matter at 6 and 3 years of age, respectively (Figure 2). Of note, while subject 1 initially showed

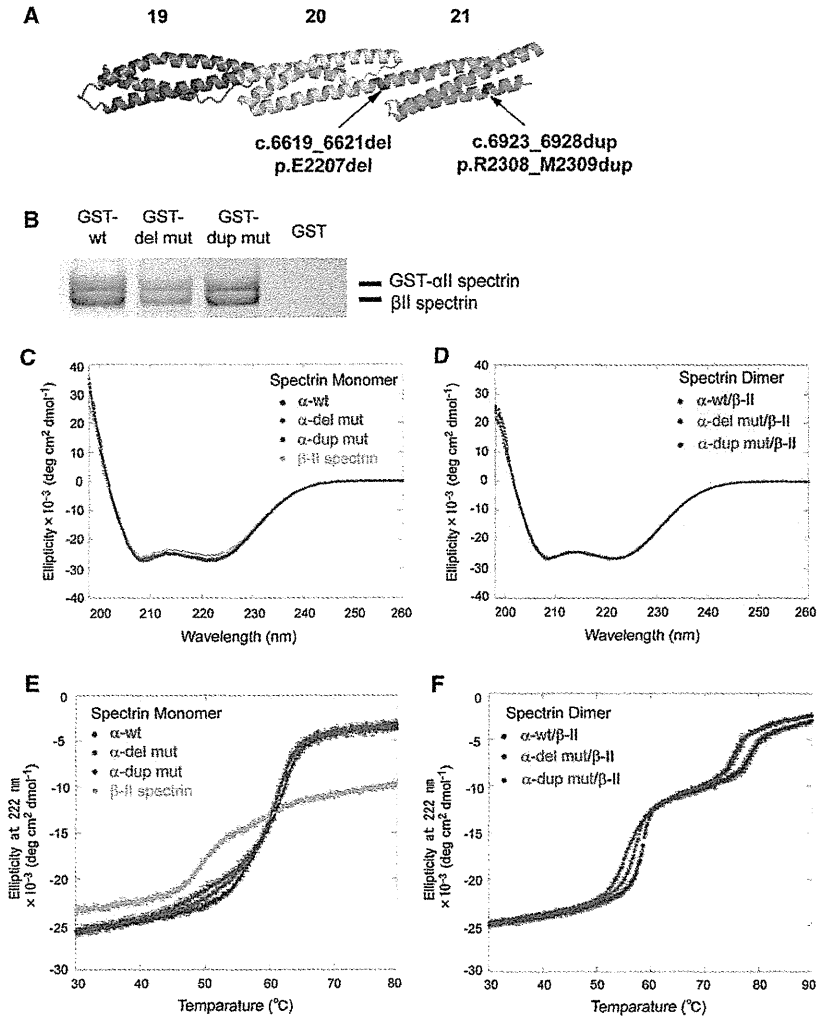

Figure 3. Mutational Effects on the α-II/β-II Spectrin Heterodimer

(A) Positions of the two mutations (c.6619_6621del, p.E2207 del in blue; c.6923_6928dup, p.R2308_M2309 dup in purple) in the predicted human α-II spectrin structure. Domains 19–21 (the last three spectrin repeats) are colored red, yellow, and green, respectively.

(B) GST pull-down assay of a recombinant GST-tagged α-II spectrin/β-II spectrin heterodimer. The WT and two mutant α-II spectrins could form heterodimers with β-II spectrin at comparable levels. β-II spectrin did not show any binding to GST alone.

(C–F) CD spectra (C and D) and CD melting curves (E and F) at 222 nm of the WT, del mut, and dup mut of α-II spectrins and β-II spectrin as a monomer (C and E) and as heterodimers of the WT, del mut, and dup mut of α-II spectrins with β-II spectrin (D and F). CD spectra showed no difference in the helical content of the WT and mutant α-II spectrin monomers and heterodimers with β-II spectrin (C and D). The WT and mutant α-II spectrin monomers are unfolded at 60°C, whereas β-II spectrin is unfolded around at 50°C (E). In contrast, dimers of WT and mutant α-II spectrins with β-II spectrin are partly dissociated and accompanied with denaturation of a local part of the monomers at 50°C–60°C (*Tm* [°C]: 58.362 ± 0.059 [WT], 55.617 ± 0.047 [del mut], 57.110 ± 0.077 [dup mut]) and completely unfolded at 70°C–80°C (*Tm* [°C]: 78.515 ± 0.327 [WT], 75.813 ± 0.115 [del mut], 75.267 ± 0.469 [dup mut]) (F). The thermostability of the heterodimers is obviously different between the WT and the mutants. Each dot represents the average of three repeated experiments; error bars, SD.

striking hypomyelination of cerebral cortex and thin corpus callosum at 12 months of age,[14] she completed myelination and showed only slightly reduced white matter at 4 years of age (Figure 2). The apparent differences of drug intractability and severity of cerebral hypomyelination and brainstem/cerebellum atrophy (subjects 2 and 3 versus subject 1) strongly suggested dominant-negative, rather than loss-of-function, effects of the in-frame mutations.

Characterization of α-II/β-II and α-II/β-III Heterodimers

The mutations were predicted to affect formation of α/β spectrin heterodimers, because they were located at the initial nucleation site of the α/β spectrin heterodimer[19] (Figures 1B and 3A). To examine the properties of the α-II spectrin mutants in the context of dimer formation, we purified recombinant WT and the two mutant α-II spectrin proteins (c.6619_6621 del, p.E2207 del and c.6923_6928 dup, p.R2308_M2309 dup, designated as del mut and dup mut, respectively). Both GST pull down and analytical gel filtration experiments revealed that the two mutants could form heterodimers with β-II spectrin at comparable levels to the WT (Figure 3B). Circular dichroism (CD) spectra indicated no difference of helical content between WT and mutant α-II spectrin monomers, nor between WT and mutant α-II/β-II heterodimers (Figures 3C and 3D). However, CD melting experiments revealed that the mutations apparently affected the thermostability of α-II/β-II heterodimers (Figure 3F). Considering the melting curves of α-II and β-II spectrin monomers (Figure 3E), the melting transitions of heterodimers in the ranges of 50°C–60°C and 70°C–80°C represent partial dissociation of heterodimers to monomers accompanied by denaturation of a local part of the monomers and complete denaturation, respectively (Figure 3F). Apparent differences of melting curves in the 50°C–60°C and 70°C–80°C ranges suggested that the mutations alter the stability of α-II/β-II heterodimers.

The effect of the mutations was further clarified by transient expression in cultured mouse cortical neurons. α-II

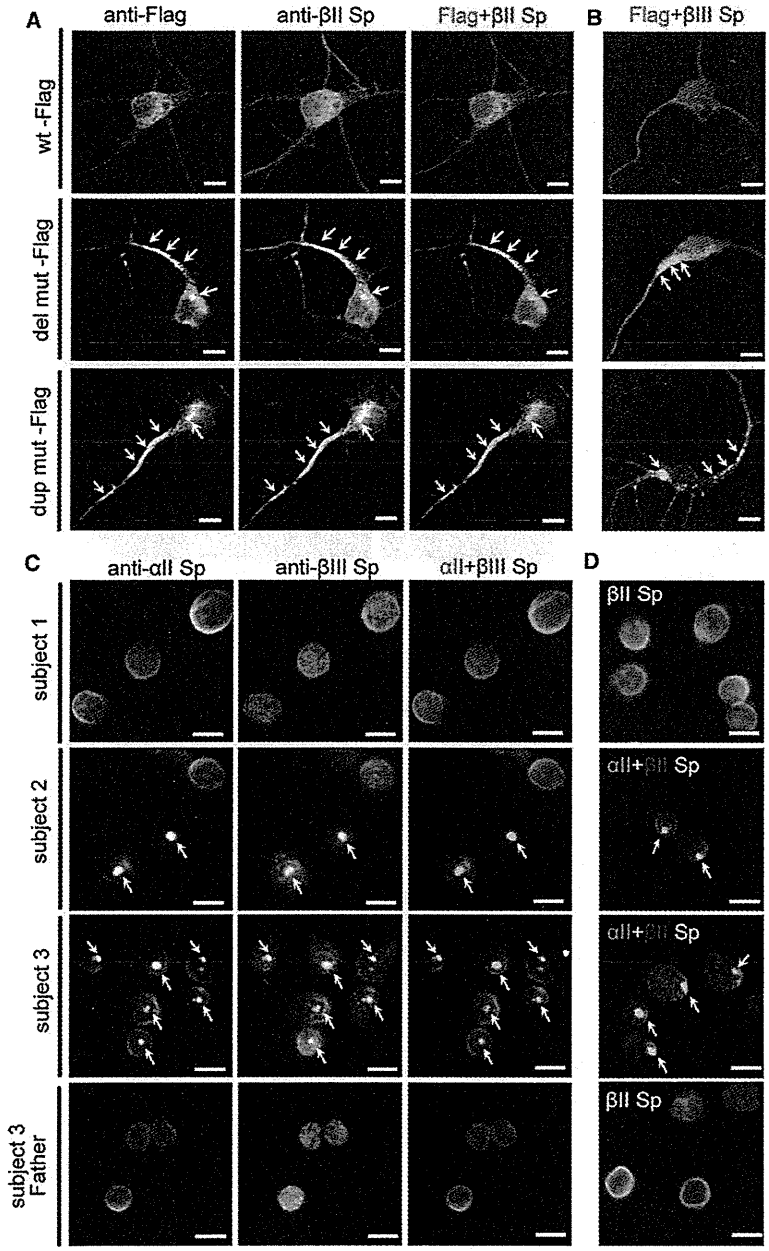

Figure 4. Mutant α-II Spectrin Causes Aggregation of α/β Spectrin Heterodimer

(A and B) Expression of the WT and the two mutant α-II spectrins at 7 DIV. Flag tagged-α-II spectrin (WT-Flag) showed similar expression to endogenous α-II spectrin (top, compare with Figure S2A). However, two mutant α-II spectrins (del mut-Flag and dup mut-Flag) showed aggregation predominantly in cell bodies and axons (arrows), and these aggregations were colocalized with β-II and β-III spectrins (middle and bottom). (C and D) Aggregation of endogenous α/β spectrin heterodimers were found in LCLs derived from two subjects harboring *SPTAN1* in-frame mutations. In LCLs of subject 2 (with c.6619_6621del, p.E2207del) and subject 3 (with c.6923_6928dup, p.R2308_M2309dup), aggregation of α-II/β-III (C) and α-II/β-II (D) spectrin heterodimers were frequently observed (middle two panels, arrows), while such aggregation was never observed in subject 1 (top). LCL of subject 3's father did not show any such aggregation (bottom).

The scale bars represent 10 μm. The following primary antibodies were used: mouse anti-α-II spectrin (1:400 dilution; clone D8B7; Abcam, Tokyo, Japan), mouse anti-β-II spectrin (1:600 dilution; clone 42/B-spectrin II; BD Transduction laboratories, San Jose, CA), rabbit anti-β-II spectrin (1:100 dilution; Abcam), rabbit anti-β-III spectrin (1:400 dilution; Abcam), mouse anti-Flag M2 (1:1000 dilution; Sigma), and rabbit anti-DDDDK-Tag (1:2000 dilution; MBL, Nagoya, Japan).

spectrin has been shown to be expressed in mouse brain, especially in neuronal axons.[20] In cultured cortical neurons, α-II spectrin was expressed at cell extensions and the periphery,[21] overlapping with the expression of β-II and β-III spectrins (Figure S2). We generated two α-II spectrin expression vectors: one was a dual expression vector of C-terminally Flag-tagged α-II spectrin and nuclear EGFP (Flag-nucEGFP), and the other was an N-terminally EGFP-tagged (EGFP) α-II spectrin. Tagged WT α-II spectrin from both vectors showed similar expression to endogenous α-II spectrin (Figure 4A and Figure S2). Notably, the two mutant α-II spectrins (del mut and dup mut) showed aggregation, predominantly in cell bodies and axons (Figure 4A, arrows, and Figure S2). Double immunostaining revealed that these aggregations were colocalized with β-II and β-III spectrins (Figures 4A and 4B, arrows, and Figure S2), indicating that unstable α-II/β-II and α-II/β-III spectrin heterodimers were involved in the aggregation. Remarkably, LCLs established from subjects 2 and 3 also showed similar aggregation, while LCLs of subject 1 and subject 3's parents showed no aggregation (Figures 4C and 4D, arrows). These findings indicated dominant-negative effects of the mutations for the integrity of α-II/β-II and α-II/β-III spectrin heterodimers. Immunostaining against β-IV spectrin did not show its involvement in the mutant aggregation (Figure S2).

Effects of the *SPTAN1* Mutations on ankyrinG and VGSC Clustering at AIS

Spectrins play important roles in clustering specific integral membrane proteins at high density in specialized regions of the plasma membrane.[8] To examine the effects of α/β spectrin heterodimer impairment, protein localization at AIS was examined, where ankyrinG and VGSC are clustered and action potentials are initiated.[22,23] At 9

DIV, expression of ankyrinG and VGSC were clustered at AIS when WT Flag-nucEGFP was transfected (Figures 5A and 5B, top). In contrast, clustering of ankyrinG and VGSC was disturbed in the presence of extensive α-II (mut)/β-II and α-II (mut)/β-III spectrin aggregation (Figures 5A and 5B, middle and bottom). Interestingly, whole-cell current clamp recordings from cortical neurons expressing mutant α-II spectrins showed impairment of repetitive action potential elicitation and elevated threshold of action potential compared with those expressing the WT (Figure 6A), while there were no significant differences in the passive membrane properties among the genotypes (Table S3). Recordings of whole-cell sodium currents with conventional activation and inactivation protocols revealed that expression of the mutants caused a significant depolarizing shift in activation compared with the WT, indicating increased threshold of sodium currents (Figures 6B and 6C). These mutants did not affect any of the activation kinetic properties (10%–90% rise time) (Figure 6E), the voltage dependence of inactivation (Figures 6F and 6G), or the whole cell capacitance (Table S3). However, peak sodium current densities were substantially reduced in cells expressing dup mut or del mut (Figure 6D). Divergent distribution of VGSC at AIS can increase the action potential threshold probably resulting from the waste of charging current across the axonal membrane;[24] therefore, the abnormal spike initiation observed in two mutants could be caused by the disturbance of VGSC clustering at AIS.

Discussion

We have shown that two de novo in-frame mutations of *SPTAN1* cause early-onset WS with spastic quadriplegia, poor visual attention, and severe developmental delay. Brain MRI of the two subjects showed severe cerebral hypomyelination, decreased white matter, widespread brain atrophy including brainstem, hypoplasia and/or atrophy of the cerebellum, and a thinned and shortened corpus callosum. On the other hand, mutations of *STXBP1* cause EIEE, and brain MRI of individuals with *STXBP1* mutations showed no structural malformations in contrast with striking structural abnormalities with *SPTAN1* mutations.[7] Among three subjects harboring *SPTAN1* aberrations, subject 1 deleted both *SPTAN1* and *STXBP1* heterozygously.[7] Similar to individuals with *STXBP1* mutations, subject 1 had distinctive features of EIEE, such as early onset of spasms, suppression-burst pattern on electroencephalogram, transition to West syndrome, and severe developmental delay.[7] Therefore it is likely that haploinsufficiency of *STXBP1* caused EIEE and subsequent WS in subject 1. However, subject 1 additionally showed apparent hypomyelination of cerebral cortex and thin corpus callosum at 12 months of age,[14] which appeared to be distinct from clinical features caused by *STXBP1* mutations. Based on these differences, we hypothesized

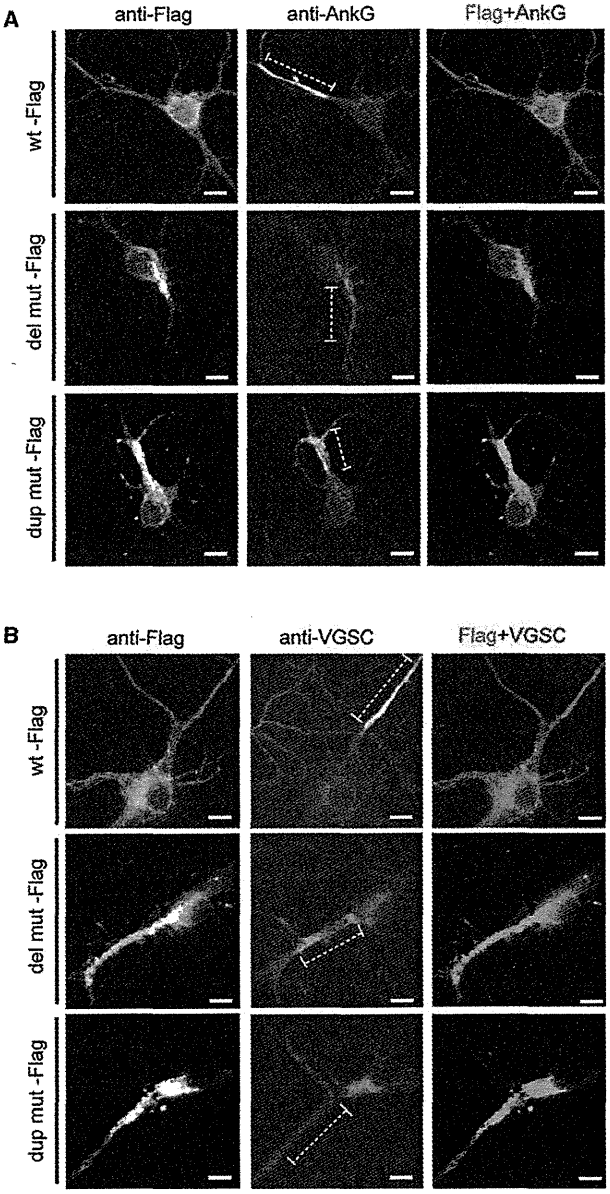

Figure 5. Transient Expression of Mutant α-II Spectrin Led to Disturbance of AnkyrinG and VGSC Clustering at AIS
Expression of ankyrinG (AnkG) (A) and VGSC (B) at 9 DIV. When WT α-II spectrin is expressed, neurons showed clustering of AnkG and VGSC at AIS (top). However, clustering of AnkG and VGSC were disturbed in the presence of extensive α/β spectrin aggregation when mutant α-II spectrins (both the del mut and the dup mut) were expressed (middle and bottom). AIS regions are shown by dashed lines. The scale bars represent 10 μm. The following primary antibodies were used: mouse anti-ankyrinG (1:100 dilution; clone 4G3F8; Santa Cruz Biotechnology, Santa Cruz, CA), mouse anti-pan sodium channel (for VGSC) (1:100 dilution; clone K58/35; Sigma), and rabbit anti-DDDDK-Tag (1:2000 dilution; MBL).

that another gene within the deletion may contribute to severe hypomyelination, and successfully found two de novo in-frame mutations of *SPTAN1* in subject 2 and 3 of

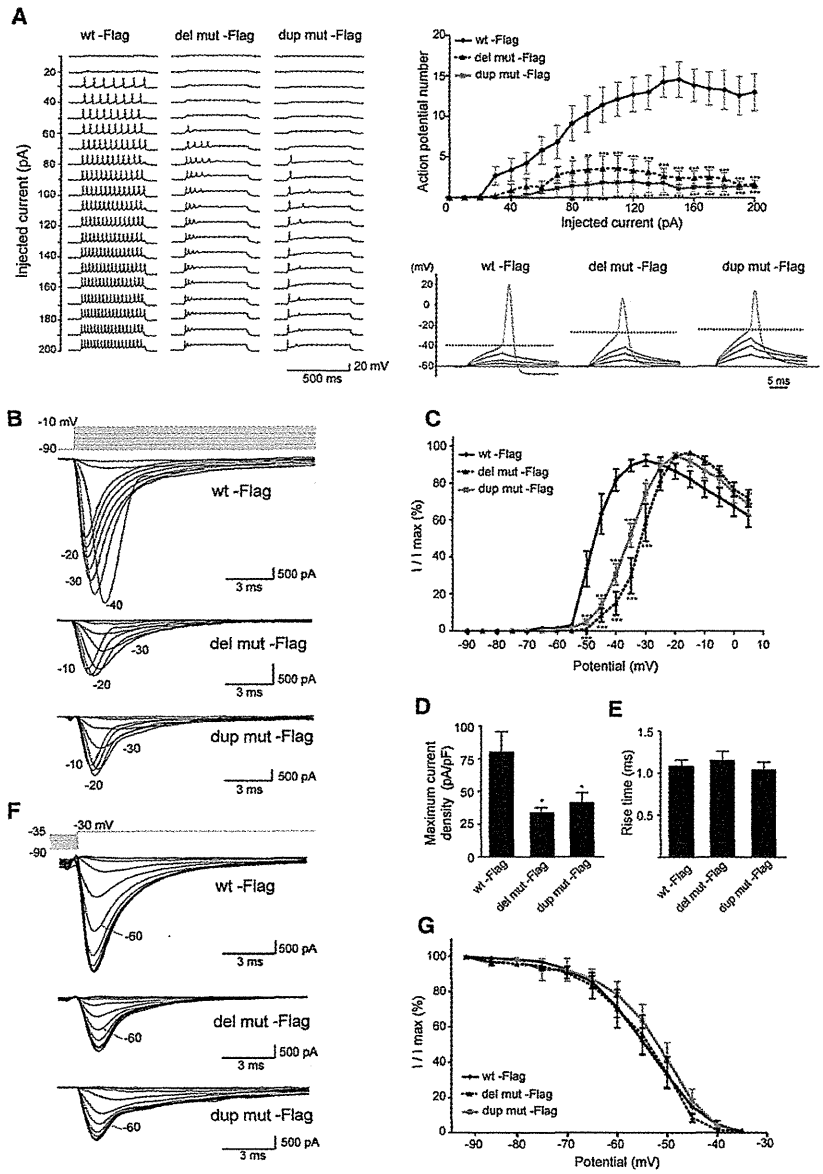

Figure 6. Mutant α-II Spectrin Elevated Action Potential Threshold in Primary Cultured Cortical Neurons

(A) Left, representative sets of action potential traces recorded from cultured cortical neurons expressing either WT or mutant α-II spectrin (del mut or dup mut)-Flag-nucEGFP during 500 ms injection of depolarizing current in +10 pA increments, from a holding potential of −60 mV. Right top, input-output relationship of the number of evoked action potentials versus the injected current (WT, n = 7; del mut, n = 9; dup mut, n = 7). Although there were no significant differences in the passive membrane properties among each genotypes (see Table S3), repetitive action potential elicitation was significantly reduced in the two mutants. Right bottom, representative responses to a series of subthreshold and suprathreshold depolarizing current injections of 10 ms duration. A base holding potential (−60 mV) and an identified action potential threshold are indicated by thin and dashed lines, respectively. Note that mutants elevated action potential threshold compared with the WT (see Table S3).

(B–G) Recordings of whole-cell sodium currents with conventional activation (C–E: WT, n = 11; del mut, n = 10; dup mut, n = 10) and inactivation protocols (G: WT, n = 11; del mut, n = 9; dup mut, n = 10).

(B) Representative sets of sodium current traces recorded from dissociated cortical neurons expressing WT and mutant α-II spectrins.

(C) Voltage dependence of channel activation measured during voltage steps between −90 and +10 mV. Statistical analysis indicated that del mut and dup mut exhibited significant differences in current-voltage relationship compared with the WT. Both mutants displayed a significant depolarizing shift in activation compared with the WT.

(D) Peak current density elicited by test pulses. Statistical analysis indicated a significant reduction in peak current in both mutants compared with the WT.

(E) Activation kinetics assessed by 10%–90% rise time plotted against test potential for WT and mutants. There were no significant differences among WT and the two mutants.

(F) Representative sodium currents in neurons expressing WT or mutant α-II spectrin under influence of 500 ms inactivation prepotentials.

(G) Voltage dependence of inactivation assessed in response to inactivating prepulses between −90 and −35 mV. Statistical analysis revealed no significant differences among WT and mutants ($p = 0.96$).

Error bars, SEM. *$p < 0.05$, **$p < 0.01$, ***$p < 0.001$, as compared to the WT. Most of the recorded parameters are summarized in Table S3.

group A. Although subject 1 initially showed severe hypomyelination, the myelination showed catch-up completion at 4 years of age. These facts suggest that *SPTAN1* hemizygosity may have temporary effects on the myelination. Further reports of microdeletions involving *SPTAN1* may give us a clear answer about the contribution of *SPTAN1* hemizygosity to hypomyelination. By contrast, subjects 2 and 3 showed more severe phenotypes than subject 1, indicating that the effect of in-frame mutations was dominant negative rather than loss of function. This idea was supported by the fact that the in-frame mutations could cause aggregation of α-II/β-II and α-II/β-III spectrin heterodimers, related to disturbed clustering of ankyrinG and VGSC at AIS. β-II and β-III spectrins have been shown to participate in stabilization of membrane proteins and axonal transport.[25,26] Although our study did not detect aggregation of the α-II/β-IV spectrin heterodimer, which is essential for stabilization of membrane proteins at

AIS,[27,28] defective α-II/β-II and α-II/β-III spectrin heterodimers might affect the stability of membrane proteins at AIS, possibly in combination with disrupting intracellular transport.

The α-II (mut)/β-II spectrin heterodimers was more unstable than the α-II (WT)/β-II heterodimers, which was manifested by CD melting experiments as differences of melting points at relatively high temperature (50°C–60°C and 70°C–80°C). In general, structural instability of proteins would lead to aggregate formation. Immunofluorescence analysis in both transiently transfected primary neuron and LCL derived from two subjects showed aggregation of α-II/β-II and α-II/β-III spectrin heterodimers, suggesting that structual instability of α-II/β-II and α-II/β-III spectrin heterodimers resulted in the aggregation.

We demonstrated a possible link between a mutant submenbranous scaffolding protein and abnormal AIS integrity. It has been suggested that the levels of ion channels at AIS are regulated by altering the cytoskeletal scaffolds.[22] A recessive mutation of scaffolding protein CASPR2 causes focal epilepsy.[29] Abnormal AIS integrity resulting from mutant α-II spectrin further underscores the importance of AIS scaffolds in the pathogenesis of epilepsy and provides new insights for WS.

Supplemental Data

Supplemental Data include two figures and three tables and can be found with this article online at http://www.cell.com/AJHG.

Acknowledgments

The authors declare no conflict of interest. We would like to thank all the patients and their families for their participation in this study. We also thank Dr. Jun-ichi Miyazaki for permitting use of CAG promoter and Dr. Sean Megason for the pCIG vector. This work was supported by research grants from the Ministry of Health, Labour, and Welfare (N.M., J.T., and M. Kato), the Japan Science and Technology Agency (N.M.), a Grant-in-Aid for Scientific Research on Priority Areas (Research on Pathomechanisms of Brain disorder) from the Ministry of Education, Culture, Sports, Science, and Technology of Japan (N.M.), a Grant-in-Aid for Scientific Research from Japan Society for the Promotion of Science (N.M. and M. Kato), a Grant-in-Aid for Young Scientist from Japan Society for the Promotion of Science (H.S.), the Research Promotion Fund from Yokohama Foundation for Advancement of Medical Science (H.S.), the Research Promotion Fund from the Uehara Memorial Foundation (H.S.), research grants from the Japan Epilepsy Research Foundation (H.S.), a grant from the 2009 Strategic Research Project of Yokohama City University (H.S.), and a research grant from the Naito Foundation (N.M.). This work has been done at Advanced Medical Research Center, Yokohama City University.

Received: March 11, 2010
Revised: April 29, 2010
Accepted: April 30, 2010
Published online: May 20, 2010

Web Resources

The URLs for data presented herein are as follows:

ClustalW, http://align.genome.jp/
dbSNP, http://www.ncbi.nlm.nih.gov/projects/SNP/
GenBank, http://www.ncbi.nlm.nih.gov/Genbank/
Online Mendelian Inheritance in Man (OMIM), http://www.ncbi.nlm.nih.gov/Omim/
Phyre, http://www.sbg.bio.ic.ac.uk/phyre/
Protein Data Bank, http://www.pdb.org/pdb/home/home.do
PyMOL, http://www.pymol.org/
UCSC Genome Browser, http://genome.ucsc.edu/cgi-bin/hgGateway

References

1. Kato, M. (2006). A new paradigm for West syndrome based on molecular and cell biology. Epilepsy Res. *70 (Suppl 1)*, S87–S95.
2. Bahi-Buisson, N., Nectoux, J., Rosas-Vargas, H., Milh, M., Boddaert, N., Girard, B., Cances, C., Ville, D., Afenjar, A., Rio, M., et al. (2008). Key clinical features to identify girls with *CDKL5* mutations. Brain *131*, 2647–2661.
3. Strømme, P., Mangelsdorf, M.E., Shaw, M.A., Lower, K.M., Lewis, S.M., Bruyere, H., Lütcherath, V., Gedeon, A.K., Wallace, R.H., Scheffer, I.E., et al. (2002). Mutations in the human ortholog of *Aristaless* cause X-linked mental retardation and epilepsy. Nat. Genet. *30*, 441–445.
4. Kato, M., Das, S., Petras, K., Sawaishi, Y., and Dobyns, W.B. (2003). Polyalanine expansion of ARX associated with cryptogenic West syndrome. Neurology *61*, 267–276.
5. Djukic, A., Lado, F.A., Shinnar, S., and Moshé, S.L. (2006). Are early myoclonic encephalopathy (EME) and the Ohtahara syndrome (EIEE) independent of each other? Epilepsy Res. *70 (Suppl 1)*, S68–S76.
6. Ohtahara, S., and Yamatogi, Y. (2006). Ohtahara syndrome: With special reference to its developmental aspects for differentiating from early myoclonic encephalopathy. Epilepsy Res. *70 (Suppl 1)*, S58–S67.
7. Saitsu, H., Kato, M., Mizuguchi, T., Hamada, K., Osaka, H., Tohyama, J., Uruno, K., Kumada, S., Nishiyama, K., Nishimura, A., et al. (2008). *De novo* mutations in the gene encoding STXBP1 (MUNC18-1) cause early infantile epileptic encephalopathy. Nat. Genet. *40*, 782–788.
8. Bennett, V., and Healy, J. (2008). Organizing the fluid membrane bilayer: Diseases linked to spectrin and ankyrin. Trends Mol. Med. *14*, 28–36.
9. Bennett, V., and Baines, A.J. (2001). Spectrin and ankyrin-based pathways: Metazoan inventions for integrating cells into tissues. Physiol. Rev. *81*, 1353–1392.
10. Ikeda, Y., Dick, K.A., Weatherspoon, M.R., Gincel, D., Armbrust, K.R., Dalton, J.C., Stevanin, G., Dürr, A., Zühlke, C., Bürk, K., et al. (2006). Spectrin mutations cause spinocerebellar ataxia type 5. Nat. Genet. *38*, 184–190.
11. Perrotta, S., Gallagher, P.G., and Mohandas, N. (2008). Hereditary spherocytosis. Lancet *372*, 1411–1426.
12. Meary, F., Metral, S., Ferreira, C., Eladari, D., Colin, Y., Lecomte, M.-C., and Nicolas, G. (2007). A mutant alphaII-spectrin designed to resist calpain and caspase cleavage questions the functional importance of this process in vivo. J. Biol. Chem. *282*, 14226–14237.

13. Voas, M.G., Lyons, D.A., Naylor, S.G., Arana, N., Rasband, M.N., and Talbot, W.S. (2007). alphaII-spectrin is essential for assembly of the nodes of Ranvier in myelinated axons. Curr. Biol. *17*, 562–568.
14. Tohyama, J., Akasaka, N., Osaka, H., Maegaki, Y., Kato, M., Saito, N., Yamashita, S., and Ohno, K. (2008). Early onset West syndrome with cerebral hypomyelination and reduced cerebral white matter. Brain Dev. *30*, 349–355.
15. Megason, S.G., and McMahon, A.P. (2002). A mitogen gradient of dorsal midline Wnts organizes growth in the CNS. Development *129*, 2087–2098.
16. Niwa, H., Yamamura, K., and Miyazaki, J. (1991). Efficient selection for high-expression transfectants with a novel eukaryotic vector. Gene *108*, 193–199.
17. Kelley, L.A., and Sternberg, M.J. (2009). Protein structure prediction on the Web: A case study using the Phyre server. Nat. Protoc. *4*, 363–371.
18. Kusunoki, H., Minasov, G., Macdonald, R.I., and Mondragón, A. (2004). Independent movement, dimerization and stability of tandem repeats of chicken brain α-spectrin. J. Mol. Biol. *344*, 495–511.
19. Speicher, D.W., Weglarz, L., and DeSilva, T.M. (1992). Properties of human red cell spectrin heterodimer (side-to-side) assembly and identification of an essential nucleation site. J. Biol. Chem. *267*, 14775–14782.
20. Riederer, B.M., Zagon, I.S., and Goodman, S.R. (1986). Brain spectrin(240/235) and brain spectrin(240/235E): Two distinct spectrin subtypes with different locations within mammalian neural cells. J. Cell Biol. *102*, 2088–2097.
21. Xu, J., Ziemnicka, D., Scalia, J., and Kotula, L. (2001). Monoclonal antibodies to alphaI spectrin Src homology 3 domain associate with macropinocytic vesicles in nonerythroid cells. Brain Res. *898*, 171–177.
22. Ogawa, Y., and Rasband, M.N. (2008). The functional organization and assembly of the axon initial segment. Curr. Opin. Neurobiol. *18*, 307–313.
23. Lai, H.C., and Jan, L.Y. (2006). The distribution and targeting of neuronal voltage-gated ion channels. Nat. Rev. Neurosci. *7*, 548–562.
24. Kuba, H., Ishii, T.M., and Ohmori, H. (2006). Axonal site of spike initiation enhances auditory coincidence detection. Nature *444*, 1069–1072.
25. Muresan, V., Stankewich, M.C., Steffen, W., Morrow, J.S., Holzbaur, E.L., and Schnapp, B.J. (2001). Dynactin-dependent, dynein-driven vesicle transport in the absence of membrane proteins: a role for spectrin and acidic phospholipids. Mol. Cell *7*, 173–183.
26. Kizhatil, K., Yoon, W., Mohler, P.J., Davis, L.H., Hoffman, J.A., and Bennett, V. (2007). Ankyrin-G and β2-spectrin collaborate in biogenesis of lateral membrane of human bronchial epithelial cells. J. Biol. Chem. *282*, 2029–2037.
27. Komada, M., and Soriano, P. (2002). [β]IV-spectrin regulates sodium channel clustering through ankyrin-G at axon initial segments and nodes of Ranvier. J. Cell Biol. *156*, 337–348.
28. Parkinson, N.J., Olsson, C.L., Hallows, J.L., McKee-Johnson, J., Keogh, B.P., Noben-Trauth, K., Kujawa, S.G., and Tempel, B.L. (2001). Mutant β-spectrin 4 causes auditory and motor neuropathies in quivering mice. Nat. Genet. *29*, 61–65.
29. Strauss, K.A., Puffenberger, E.G., Huentelman, M.J., Gottlieb, S., Dobrin, S.E., Parod, J.M., Stephan, D.A., and Morton, D.H. (2006). Recessive symptomatic focal epilepsy and mutant contactin-associated protein-like 2. N. Engl. J. Med. *354*, 1370–1377.

Disrupted *SOX10* Regulation of *GJC2* Transcription Causes Pelizaeus-Merzbacher-Like Disease

Hitoshi Osaka, MD, PhD,[1,2]
Haruka Hamanoue, MD, PhD,[3]
Ryoko Yamamoto, MSc,[4]
Atsuo Nezu, MD, PhD,[5] Megumi Sasaki, BA,[4]
Hirotomo Saitsu, MD, PhD,[3]
Kenji Kurosawa, MD, PhD,[6]
Hiroko Shimbo, MP,[1]
Naomichi Matsumoto, MD, PhD,[3]
and Ken Inoue, MD, PhD[4]

Mutations in the gap junction protein gamma-2 gene, *GJC2*, cause a central hypomyelinating disorder; Pelizaeus-Merzbacher-like disease (PMLD; MIM311601). Using a homozygosity mapping and positional candidate gene approach, we identified a homozygous mutation (c.-167A>G) within the *GJC2* promoter at a potent SOX10 binding site in a patient with mild PMLD. Functionally, this mutation completely abolished the SOX10 binding and attenuated *GJC2* promoter activity. These findings suggest not only that the *SOX10*-to-*GJC2* transcriptional dysregulation is a cause of PMLD, but also that *GJC2* may be in part responsible for the central hypomyelination caused by *SOX10* mutations.

ANN NEUROL 2010;68:250–254

Congenital hypomyelinating disorders are a heterogeneous group of central nerve system (CNS) leukoencephalopathies, most of which are inherited disorders of myelin formation. The prototype condition is Pelizaeus-Merzbacher disease (PMD; MIM312080), an X-linked disorder caused by mutations in the proteolipid protein 1 gene (*PLP1*).[1] Patients with PMD have nystagmus, impaired motor development, ataxia, choreoathetotic movements, dysarthria, and progressive spasticity. However, ~20 to 50 % of patients clinically diagnosed with PMD have no detectable abnormalities in the *PLP1* gene, and some have a distinct disease, Pelizaeus-Merzbacher-like disease (PMLD; MIM311601).

Mutations in the gap junction protein gamma-2 gene (*GJC2*, also known as *Cx47* or *GJA12*) have been reported as a cause of PMLD.[2–8] Twenty-four different mutations (8 frameshift, 10 missence, 5 nonsense, and 1 missense/insertion alterations) have been reported to date, and most if not all result in a loss of channel function.[7,9]

By combining homozygosity mapping and a candidate gene approach, we found a homozygous mutation that disrupts a SOX10 transcriptional activation site in the *GJC2* promoter region in a family showing a mild PMLD phenotype. SOX10 is an high mobility group (HMG) family transcription factor that plays a critical role in peripheral nervous system (PNS) and CNS myelination. In addition, a subset of *SOX10* mutations cause peripheral and central hypomyelination, Waardenburg syndrome, and Hirschsprung disease (PCWH; MIM609136).[10] This study reports the first case of PMLD caused by a mutation in the *GJC2* promoter and suggests that *SOX10* transcriptional regulation of *GJC2* plays a critical role in CNS myelination.

Patients and Methods

Detailed clinical information of a Japanese female patient with PMLD, who is now 25-years-old, was previously reported.[11] In brief, her healthy parents were second cousins. She had congenital pendular nystagmus as a neonate, but otherwise developed normally and was educated at a normal school. At the age of 10 years, she developed a spastic gait that worsened and made her wheelchair bound by the age of 12 years. Her disease progressed to mild athetosis of the upper limbs and ataxia by age 13 years and dysarthria by age 15 years. She cannot speak and understands only easy commands now. Brain magnetic resonance imaging at age 15 and 20 years showed diffuse hyperintensity of white matter on T2-weighted images with interval progression of brain atrophy (Fig 1). Electrophysiological examinations showed extensive nerve conduction slowing in the CNS, although this was less severe than usually seen in male patients with PMD.[11] Peripheral nerve conduction velocities were nor-

From the [1]Division of Neurology, Clinical Research Institute, Kanagawa Children's Medical Center; [2]Molecular Pathology and Genetics Division, Kanagawa Cancer Center Research Institute; [3]Department of Human Genetics, Yokohama City University Graduate School of Medicine; [4]Department of Mental Retardation and Birth Defect Research, National Institute of Neuroscience, National Center of Neurology and Psychiatry, Kodaira; [5]Division of Pediatric Neurology, Yokohama Ryoiku-iryo Center; and [6]Division of Genetics, Clinical Research Institute, Kanagawa Children's Medical Center, Yokohama, Japan.

Address correspondence to Dr Osaka, Division of Neurology, Clinical Research Institute, Kanagawa Children's Medical Center, Yokohama, 232-855, Japan. E-mail: hosaka@kcmc.jp

Additional Supporting Information can be found in the online version of this article.

Received Dec 29, 2009, and in revised form Jan 29, 2010. Accepted for publication Feb 26, 2010.

Published online in Wiley InterScience (www.interscience.wiley.com). DOI: 10.1002/ana.22022